Thorium Cycle Hybrid Reactor Design Study

EPRI

EPRI ER-1195
Project 473
Technical Report
September 1979

Keywords:
Fusion
Hybrid Reactor
Thorium Cycle
Fusion Reactor
Fusion-Fission
Tokamak Reactor

Prepared by
Westinghouse Electric Corporation
Pittsburgh, Pennsylvania

ELECTRIC POWER RESEARCH INSTITUTE

Thorium Cycle Hybrid Reactor Design Study

ER-1195
Research Project 473

Technical Report, September 1979

Prepared by

WESTINGHOUSE ELECTRIC CORPORATION
P.O. Box 10864
Pittsburgh, Pennsylvania 15236

Principal Investigator
Ronald P. Rose

Work on this study is partially sponsored by the
United States Department of Energy and the following electric utilities:

Florida Power and Light Company
Houston Lighting and Power Company
Northeast Utilities
Pennsylvania Power and Light Company
Public Service Electric and Gas Company

Prepared for

Electric Power Research Institute
3412 Hillview Avenue
Palo Alto, California 94304

EPRI Project Manager
Noel A. Amherd
Fossil Fuel and Advanced Systems Division

ORDERING INFORMATION

Requests for copies of this report should be directed to Research Reports Center (RRC), Box 50490, Palo Alto, CA 94303, (415) 961-9043. There is no charge for reports requested by EPRI member utilities and affiliates, contributing nonmembers, U.S. utility associations, U.S. government agencies (federal, state, and local), media, and foreign organizations with which EPRI has an information exchange agreement. On request, RRC will send a catalog of EPRI reports.

NOTICE

This report was prepared by the organization(s) named below as an account of work sponsored by the Electric Power Research Institute, Inc. (EPRI). Neither EPRI, members of EPRI, the organization(s) named below, nor any person acting on their behalf: (a) makes any warranty or representation, express or implied, with respect to the accuracy, completeness, or usefulness of the information contained in this report, or that the use of any information, apparatus, method, or process disclosed in this report may not infringe privately owned rights; or (b) assumes any liabilities with respect to the use of, or for damages resulting from the use of, any information, apparatus, method, or process disclosed in this report.

Prepared by
Westinghouse Electric Corporation
Pittsburgh, Pennsylvania

ABSTRACT

This report discusses the progress made on the study of thorium-uranium fuel cycles in a tokamak hybrid reactor and on cost improvement considerations such as the use of a bundle divertor for impurity control. The thorium fuel cycle offers the potential for greater proliferation resistance than the previously studied plutonium-uranium fuel cycle. The initial effort in the neutronic blanket analyses (1) evaluated alternative blanket arrangements to assess the ^{233}U fissile fuel production capability of the hybrid, (2) determined tritium breeding capabilities of various blanket zone arrangements, (3) established that plutonium production can be controlled by design parameter selection to either breakeven or burnup ^{239}Pu, and (4) calculated the associated thermal power output for each of the scenarios. It was concluded that the hybrid could produce 1 to 4 tonnes/yr of ^{233}U with the various designs considered. Further study would be required to select an optimum design for a completely self-sufficient plant. A preliminary bundle divertor concept was completed and analyzed which showed an improved performance over previous concepts. Cost considerations are discussed, but overall plant cost analysis was not conducted since the study consisted of parametric analysis and subsystem design considerations.

Blank Page

EPRI PERSPECTIVE

PROJECT DESCRIPTION

This is a project investigating the feasibility of fusion-fission applications based on projections of late 1980's tokamak plasma physics and technology.

The results of an assessment of actinide burning conducted in the first year of project activities have been reported in EPRI report ER-451 (Volumes 1 and 2). Results of an assessment of plutonium production conducted during the second year of project activities are described in EPRI report ER-1083 (Volumes 1 and 2). The present report describes the potential for production of fissile uranium from thorium.

PROJECT OBJECTIVES

The objectives of the activities reported herein were to provide a preliminary estimate of the technical potential of producing fissile uranium using 1980's technology and beam-driven tokamak fusion reactors and to investigate in greater depth the feasibility of cost improvements in tokamak hybrid reactors.

PROJECT RESULTS

The results of this investigation show that near-term, beam-driven tokamak fusion-fission devices could produce abundant amounts of ^{233}U. Depending upon the details of the blanket design, ^{233}U production rates between 1.5 and 4 tonnes per year appear feasible. Important factors affecting this variation are tritium production rates, blanket neutron multiplication, and the desired amount of blanket thermal power. The larger values of ^{233}U production require blanket neutron multiplication.

In addition, design concepts have been developed for a tokamak with a bundle divertor. As well as providing for a reactor cost decrease, the compact form of the bundle divertor allows better blanket coverage for improved fusion neutron utilization.

While this study indicates the plausibility of ^{233}U production and for major cost reductions in tokamak reactors, estimates of the reactor design, performance and economic characteristics will have to be developed from subsequent, more-detailed investigations.

Noel A. Amherd, Project Manager
Fossil Fuel and Advanced Systems Division

ACKNOWLEDGMENTS

This study was conducted as an interdisciplinary effort which involved several principal contributors with their primary areas of responsibility as follows:

Neutron Wall Loading in Toroidal Geometry	D. L. Chapin
Poloidal Field Coil Analysis	H. R. Howland
Nuclear Design and Analyses	J. Jedruch
Nuclear/Thermal-Hydraulics Analyses	J. R. McCown
Costing Considerations; Editing	J. L. Kelly
Program Objectives	R. P. Rose
COAST Code Summary	D. A. Sink
Plasma Engineering Considerations	E. W. Sucov
Bundle Divertor Design and Analysis	T. F. Yang

Blank Page

TABLE OF CONTENTS

Blank Page

ILLUSTRATIONS

TABLES

1.0 INTRODUCTION

The development of near-term applications of energy technologies such as hybrid tokamak reactors has become of immediate interest to utilities and the government. In addition, concerns with respect to the possible diversion of fissile materials for weapons use have prompted an interest in the thorium fuel cycle. The alternative Th-U fuel cycles are combined in this study with a potentially attractive tokamak impurity control concept - the bundle divertor. This work evaluates both of these concepts and is a natural extension of the earlier hybrid and actinide burner studies conducted at Westinghouse. The previous hybrid study concentrated on breeding plutonium from ^{238}U.

Thorium Fuel Cycle

The goals and objectives of the thorium fuel cycle aspect of the study involve re-examining the Th-^{233}U cycle in view of the large thorium resources available and concerns regarding diversion. This examination requires that an assessment be made in two areas: (a) Breeding ^{233}U in a hybrid tokamak reactor; and (b) Characterizing the fission reactor "market" for ^{233}U.

Breeding ^{233}U in a tokamak hybrid reactor requires the evaluation of what neutron multiplication is needed to increase the production rate of fissile material and which trade-offs should be examined with respect to fuel production and power generation to identify the best mix to minimize total costs. Section 5 of this report discusses the results of these studies.

The "market" for Th-^{233}U must also be addressed by characterizing the spectrum of fission reactors that are potential users for this fuel. Reactor concepts considered to date for use with the Th-^{233}U fuel cycle include the HTGR, LMFBR and CANDU reactors. These are all examples of present or near-term fission technology. If an adequate source of ^{233}U is available, however, a much broader set of fission reactor options appears possible. These include an LWR burner

with "denatured" ^{233}U and an LWR "near breeder" where some of the neutronic constraints of the LWBR are relaxed. The potential fuel cycle scenarios will be addressed by other studies and are not a part of this report.

Bundle Divertor Concept

A divertor acts as an exhaust system, which is needed for a long pulse, beam driven tokamak to remove leaked fuel, impurities, and ash from the plasma area. The conceptual designs for both the actinide burner and the Pu-U hybrid breeder have incorporated a poloidal type divertor. This type of divertor required a total exhaust flow area of approximately 30 m^2 to carry the particles out of the system. While other approaches were considered early in the Pu-U fuel cycle hybrid reactor study, none were identified that could provide a significant reduction in this exhaust flow area. Recent experimental results from the DITE tokamak at the Culham Laboratory in England, however, indicate an alternative. The DITE tokamak incorporates a "bundle divertor" which appears to have the capability of reducing the exhaust flow area for a tokamak to $\sim$1 m^2. This reduction in flow area is possible because of a significantly higher particle density in the exhaust stream. A comparison of divertor concepts is shown in Figure 1-1.

A bundle of particles is drawn from a scrape-off layer past the toroidal stagnation point to a collector system by divertor coils which oppose the toroidal field system. Since these exhaust particles are carried completely out of the tokamak system by this approach, the particle collection system could conceivably recover the energy from these exhaust particles in the form of electricity by a direct conversion system. However, there is a significant design concern in incorporating a bundle divertor. The divertor coils have to "buck" the main toroidal field. The forces on these windings can therefore be very large. Preliminary calculations were performed which indicate that, by moving the divertor coils close enough to the plasma and keeping the divertor aperture small enough, the magnetic forces can be reduced to a point where restraining the coils appears feasible.

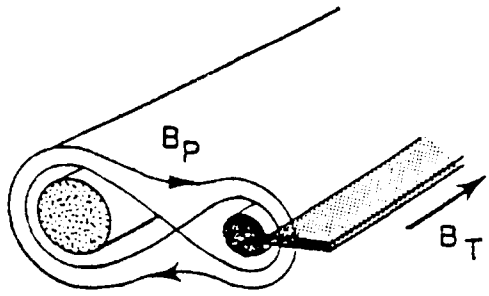

POLOIDAL DIVERTOR

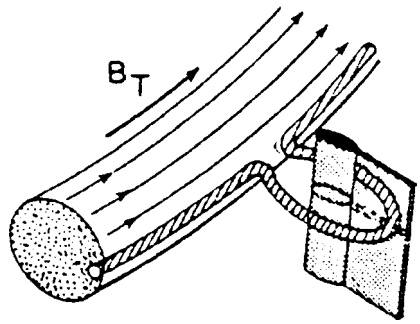

BUNDLE DIVERTOR

Figure 1-1. Comparison of Divertor Concepts

The advantages and disadvantages of the bundle divertor when compared to systems with a poloidal divertor, are as follows:

Advantages	Disadvantages
• Possible reduction in vertical size of tokamak	• Divertor coils experience large forces
• Exhaust carried completely out of the torus where collection problems are much easier to solve	• Minimum shielding space for divertor coils is available
• Plasma exhaust with small flow area required	• Larger power consumption may be necessary for divertor
• Divertor is energized with toroidal field magnet system, eliminating cycling with poloidal field coils	• Larger space required between TF coils, which may require larger or fewer TF coils
• More predictable plasma current initiation may be possible	
• May eliminate liner, thus reducing structure between plasma and blanket lattice	

The advantages of the bundle divertor shown in the above tabulation are indeed significant and the disadvantages do not appear to be insurmountable. Therefore, the bundle divertor appears to be a very attractive concept by which to effect significant reductions in capital cost and improvements in performance for a tokamak reactor. Section 4 of this report discusses the technical evaluation of the bundle divertor. A general discussion of economic considerations is presented in Section 3.

2.0 SUMMARY AND CONCLUSIONS

Work was initiated on the thorium fuel cycle tokamak hybrid reactor study by performing parametric studies of various thorium fuel cycles and means of reducing capital costs by incorporation of a bundle divertor. In addition, considerable effort has been expended to examine the issue of nuclear proliferation as it relates to fusion power. This latter work was performed at the request of ERDA and has been reported separately.[1]

Preliminary parametric studies of fusion driver parameters to identify approaches which will improve system economics were initiated with the objective to improve performance (moving nearer to ignition by increasing β, field on axis, and/or elongation), to increase fusion power density and to reduce recirculating power (i.e. increase Q). These changes are representative of projections to a commercial fusion-fission system, as opposed to a demonstration reactor. The potential range of parameters identified for these studies is as follows:

$$2.0 \leq Q \leq \infty \text{ (ignition)}$$
$$7\% \leq \beta_t \leq 10\%$$
$$4T \leq B_t \leq 7T$$
$$4.5\,m \leq R_o \leq 6.0\,m$$
$$0.9\,m \leq a \leq 1.5\,m$$
$$1.6 \leq b/a \leq 2.0$$
$$2\ MW/m^2 \leq \Phi_w \leq 6\ MW/m^2$$

Algorithms are being developed for incorporation in the COAST Computer Code to cover the range of plasma physics conditions associated with the above parameters and to modify the geometric constraints to describe a fusion-fission tokamak system (e.g. to add the algorithms required for a fertile/fissile blanket).

Work was performed on the bundle divertor in parallel with the above parametric effort. This work is directed toward overcoming some of the inherent difficulties

of the bundle divertor, such as large coil forces as applied to the hybrid tokamak geometry. Since the current carried by the coils of the bundle divertor is proportional to the toroidal field and only a small bundle of toroidal flux is diverted, the current in the divertor is inherently large, its interaction with the toroidal field is very strong, and the particle collection surface area available is small. In addition, the space available for shielding is small and not of uniform thickness. The objective of this effort was to find solutions for these problems. A significantly improved design was developed.

The first significant improvement was that the diverted fluxes were swept outside the tokamak through the gap between two adjacent TF coils. In this manner, the fluxes can be expanded, the collection problem is relieved, and the forces on the part of coil inside the TF bore are much reduced. However, high current density magnet technology is still required to keep the conductor area small. A significant effort has been required to find a method to increase the shielding space without causing a severe perturbation to the plasma. The second significant improvement was development of an approach leaving room for shielding by adding a pair of vertical coils on the plane passing through the center line of the divertor. This coil pair will modify the toroidal flux locally in the region of the separatrix loop. Thus, the shielding space is increased and the shield thickness becomes uniform. The coil forces are further reduced by this approach. The same method can be applied to the other part of the divertor coil and to the flux expansion windings. Figure 2-1 shows the trimetric view of such a design. The loss of alpha particles due to field ripple has been determined by a preliminary analysis to be <1%. The shielding and the high current density magnet technology have yet to be evaluated. Further iteration in the analysis is required when more specific reactor size and plasma parameters are defined.

Blanket parametric studies of the thorium fuel cycle were initiated using a multiple-region blanket, 1 m thick, with 30 cm allowed for coolant plenum and manifolds. The blanket fuel section thickness of 70 cm was divided into three zones: the fast neutron multiplying zone loaded with U, PuC; the ThC loaded breeding zone; and the tritium breeding zone containing Li_2O. The combined width

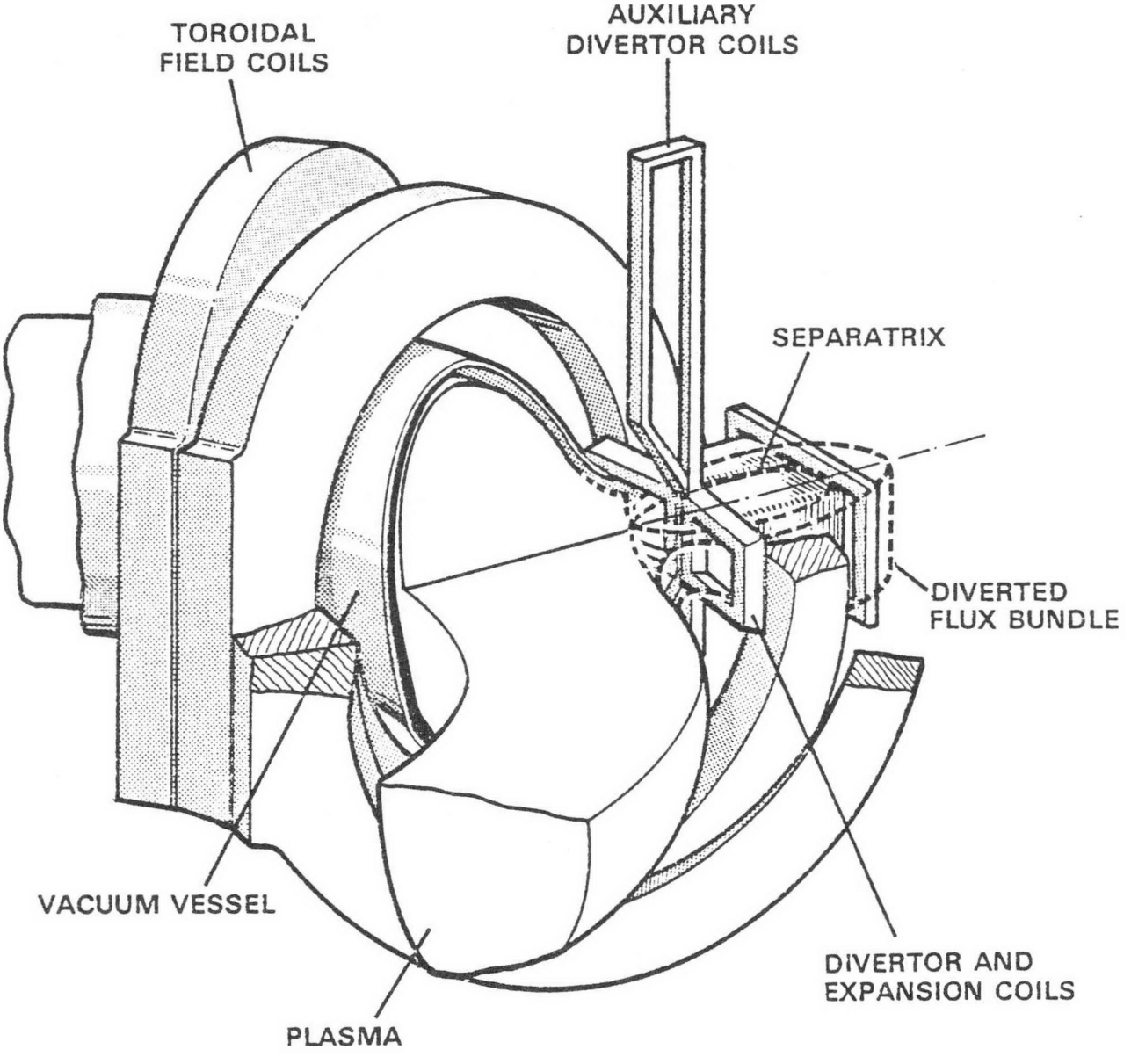

Figure 2-1. Trimetric View of a Bundle Divertor Design

of the first two zones was initially fixed at 50 cm and 20 cm was allocated to the tritium breeding zone. The layout of these zones is shown in Figure 2-2. Plutonium in the neutron multiplying zone was assumed to be that discharged from an LWR with 69.6% ^{239}Pu and 30.4% ^{240}Pu. Should the availability of Pu become a problem due to restrictions imposed on fuel reprocessing, blankets enriched in ^{235}U or self-generated ^{233}U could be used. In the latter case, there is generally a penalty imposed on the performance of the blanket for an initial period of several years, until the inventory of ^{233}U bred in the blanket builds up to a significant level.

Highlights of the results of these parametric calculations are presented in Table 2-1 for beginning of life (BOL) conditions where most cases studied used TZM clad fuel, helium coolant and assumed an optimistic (future commercial application) 4 MW/m^2 source at the first wall. These data show that significant production (>1.5 tonnes/year) of ^{233}U is feasible. Adequate blanket thermal power (3 GW_t will achieve electric power breakeven) can be obtained with proper choice of parameters. Self-sufficient tritium breeding can be achieved, but is difficult with a toroidal geometry and normal thermal power (3 GW_t). The net ^{239}Pu production can be controlled, since zero net Pu production is an objective. Finding a point design to achieve all of these goals at once within near-term technological, economic and environmental constraints appears difficult.

Group A, case 1 in Table 2-1 indicates a ^{233}U production of $\sim$3.7 tonnes/year, while Pu-production is only $\sim$0.5 tonnes/year. This concept requires no initial Pu inventory, i.e., a 2 cm thick UC neutron multiplier zone with a 48 cm ThC breeding zone is employed. However, the thermal power (1.2 GW) is inadequate and tritium breeding ratio is less than half the required amount ($\sim$1.2). Enriching with Pu (10%) in a thicker multiplier zone (6 cm) resolved the thermal power deficit, but resulted in increased Pu production and still had inadequate tritium breeding as shown in case no. 8. Hence, further parametric study to increase tritium breeding and reduce Pu production was conducted.

Group B, case 8 in Table 2-1, indicates that the required T-breeding ratio can probably be achieved by higher enrichment with Pu, but the resulting performances are not clearly compatible with near future technology. The 10 cm thick neutron multiplier zone has 15 a/o Pu in the U, PuC and the rather thin (10 cm) thorium zone was also enriched (5 a/o Pu). The Li_2O zone is 35 cm thick. The fuel rod

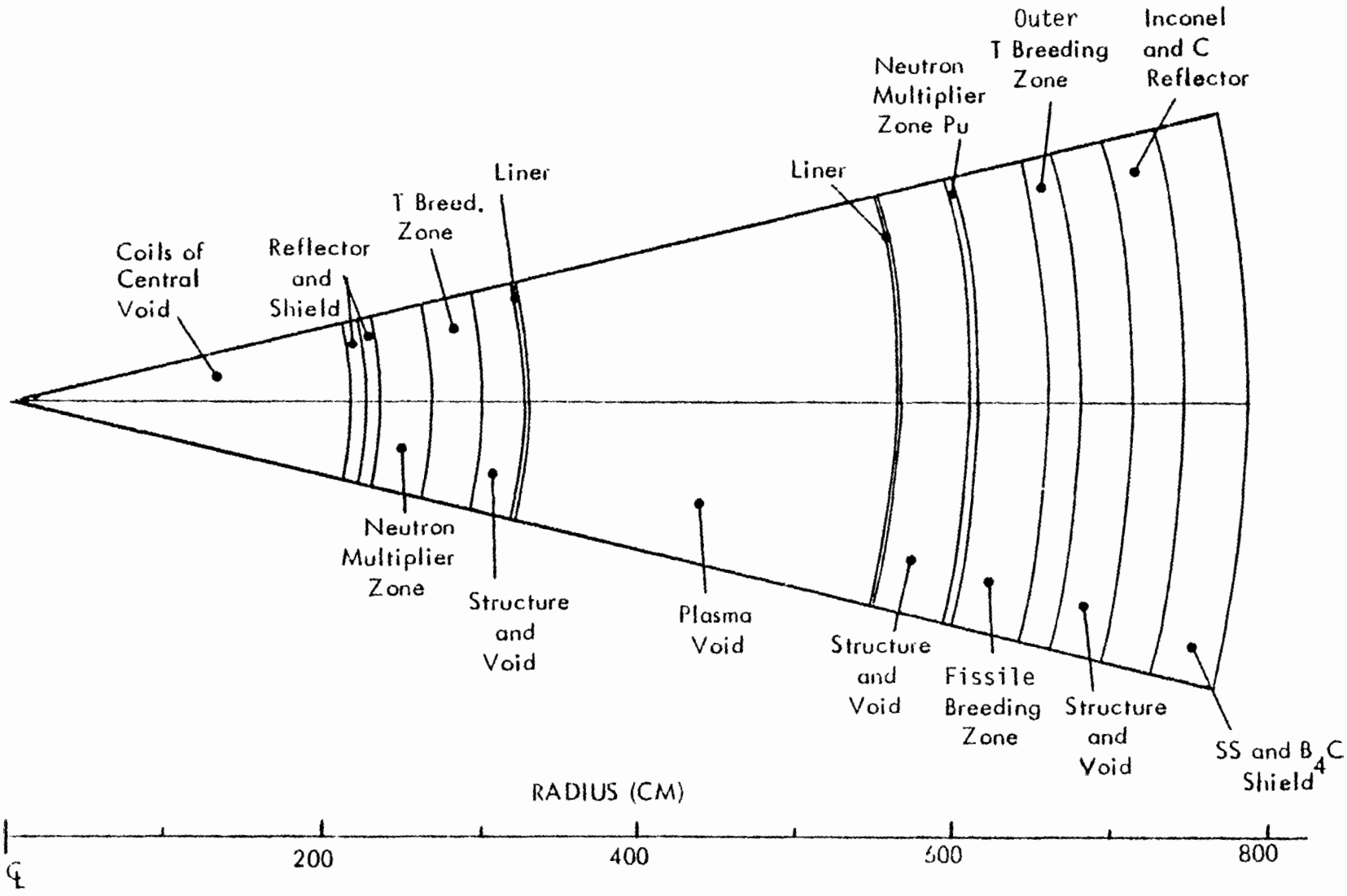

Figure 2-2. Top View of the Simplified Geometry Model Used in Blanket Scoping Calculations

TABLE 2-1

HIGHLIGHTS OF BLANKET PARAMETRIC CALCULATIONS

	Case No.	Blanket Zone/Width, (a)/(cm)			Pu Enrichment, a/o P_u(b)	Initial Inventory, tonnes			Tritium Breeding Ratio	Fissile Production, BOL-(tonnes/year)(e)		Blanket Thermal (e) Power (BOL) (GW)
						Pu	U	Th		^{233}U	^{239}Pu	
Group A		(U,PuC)	(ThC)	(Li_2O)	(NM)							
(^{233}U Breeder)	1	NM/2	FB/48	TB/20	0	0	30	620	0.44	3.7	0.5	1.2
	8	NM/6	FB/44	TB/20	10	9.1	82	570	0.51	3.9	0.6	4.1
	9	NM/10	FB/40	TB/20	10	15.2	137	520	0.56	3.8	1.2	6.6
Group B (d)		(U,PuC)	(ThPuC)(c)	Li_2O C								
(U&T Breeding Power Plant)	6	NM/15	FB/5	TB/35 15	10	26.9	206	72	1.03	1.1	2.0	13
	8	NM/10	FB/10	TB/35 15	15	30.7	130	143	1.08	2.8	-0.5	15
	9	NM/15	FB/5	TB/35 15	15	38.4	196	72	1.50	1.7	0.1	25
Group C		(Li,40% Li-6)	(U,PuC)	(ThC)								
(U&T Breeding)	14	TB/20	NM/10	FB/40	15	24	134	637	1.11	1.2	0.0	2.9
Group D		(Li/Li6)	(ThPuC)	(ThC)				(FB/NM)				
(Pu Convertor-U&T Breeding Power Plant)	5	TB/10 (37% Li-6)	NM/10	FB/30	30	46.6	---	572/105	1.20	4.6	-2.8	9.1
	9	TB/14 (40% Li-6)	NM/6	FB/30	35	32.8	——	572/59	1.11	3.3	-2.4	4.3
	15	TB/14 (24% Li-6)	NM/6	FB/30	41	38.4	——	572/53	1.18	4.1	-4.1	7.2

(a) Zones are NM-neutron multiplier; FB - Fissile Breeding; TB - Tritium Breeding. Order listed is closest to plasma first and then outward sequence. The fusion power source density is assumed to be 4 MW/m^2 at the first wall for all cases.

(b) Pu is assumed to be 69.6% fissile from LWR discharge.

(c) Pu is enriched to 5 a/o in Th,PuC.

(d) This group uses stainless steel clad in lieu of T/M.

(e) These values are at 100% plant capacity factor.

clad was changed from TZM to 316 stainless steel. The ^{233}U production of ∿2.8 tonnes/year and the Pu consumption of ∿0.5 tonnes/year would be satisfactory, but the high Pu initial inventory (∿31 tonnes) and high thermal power (15 GW_t will net ∿3 GW_e) may not be compatible with probable fuel processing and power conversion technologies of the year 2000. The fuel rod power density was 1520 W/cm^3. Thus, it appears that achieving tritium self-sufficiency in a toroidal geometry with tritium breeding in the inner torus and outer edge of the outer torus area may be difficult unless high thermal power (∿13 GW) is achieved or highly enriched fuel is used.

An alternative for achieving the required tritium breeding is shown as group C, case 14 in Table 2-1. In this concept, a 20 cm thick lithium zone was placed adjacent to the plasma followed by a 10 cm U, Pu (15% enriched) C neutron multiplier zone and a 40 cm ThC breeder zone. This concept achieved marginal T-breeding and thermal power, low ^{233}U breeding, and no Pu production, but required significant Pu enrichment. It appears that further optimization of this concept could achieve satisfactory tritium breeding, better ^{233}U production and the thermal power. Evaluation of an Li_2O zone (30 cm) next to the plasma followed by a narrow neutron multiplier zone and then a thicker thorium breeder zone may be worth pursuing, particularly if the fuel clad is changed to less absorbant stainless steel in lieu of TZM, as was done in Group B.

An alternate use of the hybrid reactor as a "Plutonium Convertor" was given a cursory evaluation. This concept assumes that ample Pu is available from LWR discharge and a need exists to "burn up" the material rather than store it or recycle it. The data shown as group D in Table 2-1 summarizes the performance potential of the Pu convertor. Cases number 5, 9, and 15 show that inventories of ∿33 to 47 tonnes of Pu can be burned up at rates of ∿2.4 to ∿4.1 tonnes/year while producing ^{233}U at rates of 3 to 5 tonnes/year with thermal power outputs of 4 to 9 GW. Tritium breeding self-sufficiency was achieved with little difficulty using ∿24 to 40% Li-6 in the Li zone next to the plasma.

In addition to these neutronic parametric studies, work has been completed to provide a better prediction of the spatial distribution of 14 MeV neutron current

incident on the first wall. A program which calculates the variation of the neutron wall loading about the first wall of an axisymmetric fusion reactor has been implemented. A version for a rectangular shaped wall has been checked and is operating properly. Modifications were made to enable the code to handle an elliptical shaped wall and plasma. The wall loading variation can be determined for up to three plasma source distributions: uniform, peaked, or peaked and outwardly shifted. The results from this code are used to determine what fraction of the fusion neutrons strike the inner wall of the torus, where there may not be a breeding blanket. It is also used to determine the peaking of the wall loading on the outer wall, which is important from radiation damage considerations. The poloidal variation of the wall loading is useful in determining such quantities as the fraction of the neutrons striking a particular wall section and the amount of peaking in the wall load at various "hot spots". Results of the analysis indicated that about 55% of the neutrons strike the outer blanket, while about 20% strike the top and bottom areas and about 25% penetrate the inner blanket. It was also found that the wall loading at the outermost wall position is about 40% above the average, which will have significant effects on the cooling requirements and radiation damage at that point.

3.0 COST IMPROVEMENT CONSIDERATIONS

The purpose of this section is to examine available options such as revising plasma parameters to reduce the cost of producing fissile fuel in a hybrid reactor and define other alternatives that would result in a more economical commercial hybrid reactor.

The high estimated capital cost for hybrid reactors and high unit cost of Pu are motivation to find ways to reduce cost of Pu. Original design goals set by Westinghouse and EPRI on previous studies limited technology to the mid-1980s and focused on breeding using natural fertile materials. This resulted in a design with fairly conservative plasma physics and a blanket designed for fissile breeding. However, competitive economics make it necessary to consider a mature commercial plant operating in the first decade of the 21st century. Therefore, it can be assumed that significant improvements are possible in the evolution of mature fusion-fission technology. In order to improve the unit cost of the fuel, several strategies are possible: reduce capital cost of the plant; make more fissile fuel; sell electric power. Capital cost reduction can come from simplifying or removing some of the systems in the original design such as reducing neutral beam power requirements, or using a bundle divertor instead of the poloidal divertor. Increased fissile fuel production could come from an optimized blanket design, higher first wall loadings and less parasitic structure. Selling electric power will be possible if: a) more electric power is generated; and b) less circulating power is needed to run auxiliary systems such as the neutral beam lines and coolant circulating systems.

Some approaches that could lead to cost reduction and performance improvement are:

- New or improved design concepts, perhaps involving relaxation of assumed constraints
- Improved plasma parameters

- Device sizing so as to make the best use of a given set of design concepts

- Changes in costing approach such as smaller contingencies and the use of learning curve effects for commercial applications

Some of these approaches are discussed in the following subsections.

3.1 DESIGN CONCEPT ALTERNATIVES

Several specific departures from the TCT Hybrid Reactor Concept[4] were designated that could provide more economic feasibility for future applications. Among these were:

- Increasing plasma Q, so as to reduce circulating power (see subsection 3.2)

- Enriching the blanket to achieve greater blanket power production (see subsection 5.2)

- Incorporating a bundle divertor with possible reduction in toroidal field coil size, and probable direct energy recovery (see section 4.0)

- Incorporating more conventional blanket technology to be more compatible with LWR fuel interfacing, thereby reducing developmental risks

- Incorporating an ignited plasma option which may achieve higher power densities which could increase blanket performance

- Continued cost trade-off studies such as the evaluation of vertical neutral beam injection schemes to maximize space available for the fertile blanket and reduce costs (see subsection 3.5)

- Optimistic future-of-the-art material performance criteria will be used. (12 MW-yr/m^2 integrated fluence-exposure lifetime for vessel wall)

- Success in the development of the negative ion source neutral beam injection system will be assumed.

- A mature, reactor design will be assumed, i.e., development costs of the first-of-a-kind items will not be charged to the project.

- Recovery and reprocessing of either Pu or ^{233}U from spent fuel will be assumed commercially available and fully licensed.
- The plant will be required to generate its own replacement T inventory, i.e., a tritium breeding ratio of almost 1.2 will be needed.
- An energy conversion system of sufficient thermal inertia to allow pulsed tokamak operation to be converted into continuous power feed into the commercial grid will be required. That is, excess power is assumed saleable.
- The requirements of T-breeding from previous studies indicate that the introduction of a Li zone (solid Li compounds in vented pins, etc.) in the outer blanket is necessary unless high thermal power, i.e. enriched fuel in fissionable blanket, ($\sim$10 - 15 GW_t) is achieved.

Although all of these items were not evaluated during this study, the above concepts were considered with respect to decisions made on the approaches that were evaluated.

3.2 PLASMA PARAMETERS

Possible improvements in plasma physics parameters were considered with the goal of increasing both Q and the first wall loading. The maximum Q of infinity can be achieved in an ignited plasma using high B_t. The ignited hybrid may have an inherent economic advantage over an ignited pure fusion reactor due to higher power density. Thus, the hybrid could generate electricity for sale and produce fissile fuel as a salable product as well, provided reliability and availability requirements for electrical generation could be achieved.

It has been suggested that a Q = 2.5 hybrid plasma may be the minimum for a commercial system (see Table 3-1 for definition of nomenclature). Some scaling relations are: $n\tau \propto n^2a^2$, $nT \propto \beta B^2$, and $\phi_w \propto n^2 \sigma v a$. Since it is assumed that σv is fixed, $\phi_w \propto n^2a$. In order to get Q = 2.5, $(n\tau)_{2.5}$ must equal 8×10^{13}. The previously studied TCT hybrid reactor with Q = 1.25 has $(n\tau)_{1.25} = 2 \times 10^{13}$; therefore, $(na)_{2.5} = 2\ (na)_{1.25}$. Choosing to make the major increase in "n" rather than "a" results in the parameters in Table 3-2.

Thus, increasing Q generates a higher wall loading ϕ_w, at the expense of a higher field on axis, B_t, and greater neutral beam energy, W_b. An ignition device

TABLE 3-1

DEFINITION OF SYMBOLS

Q	=	ratio of fusion power generated in the plasma to the injected neutral beam power
B_t	=	magnetic field on plasma axis
R	=	major radius of tokamak
a	=	minor horizontal radius of plasma
b	=	minor vertical radius of plasma
β	=	ratio of plasma pressure to the confining magnetic field
ϕ_w	=	fusion neutron wall loading
n	=	fuel ion density in the plasma
τ	=	energy confinement time of the plasma
T	=	average plasma temperature
σv	=	fusion reaction rate coefficient
W_b	=	neutral beam energy

TABLE 3-2

ESTIMATED HYBRID PLASMA PARAMETERS WITH INCREASED Q

	Q = 1.25	Q = 2.5	Q = 2.5
$n\tau \propto (na)^2$ $(s\text{-}cm^{-3})$	2×10^{13}	8×10^{13}	8×10^{13}
n (cm^{-3})	1×10^{14}	2×10^{14}	1.8×10^{14}
a (m)	0.9	0.9	1.0
R (m)	4.45	5.0	5
$\phi_w \propto (n^2 a)$ (MW/m^2)	1.55	5.6	5.5
T (keV)	6.5	8	6.5
β (%)	5.5	7	5.5
$B_t \propto \left(\frac{nT}{\beta}\right)^{1/2}$ (Tesla)	4.2	5.9	5.6
W_b (keV)	200	400	360

similar to the TNS-4 parameters shown in Table 3-3 could be considered as the plasma parameters of a commercial hybrid reactor. The COAST code has capability for comparing costs of various tokamak point designs and therefore, it can be used to examine plasma parameters within the desired limits. The range of plasma limits to be evaluated was chosen as:

$$2.0 \leq Q \leq \infty$$
$$4.5 < R_o < 6\ m$$
$$0.9 < a < 1.5\ m$$
$$1.6 \leq b/a \leq 2.0$$
$$7\% < \beta < 10\%$$
$$4\ T < B_t \leq 7\ T$$
$$2\ MW/m^2 \leq \phi_w \leq 6\ MW/m^2$$

The bundle divertor was previously identified as having potential for increased performance with reduced capital costs. However, the bundle divertor has several problems: a) very large forces on divertor coils; b) potentially large power consumption in coils; c) confinement of alphas may be decreased; and d) very high current density is required. The forces on the coils can be reduced if the coil bore is reduced. Therefore, it was considered that limiting the bore to a size just large enough to remove alphas at the same rate as they are being created may be a viable approach. Another approach is not to use a divertor at all and: a) allow plasma to burn until it quenches due to either alpha or impurity buildup; b) assume alphas diffuse out of the plasma at same rate as do the fuel ions and can be pumped away by a vacuum system. (However, this approach was evaluated on the Actinide Burner Study and found not feasible.) Examination of these possibilities may be fruitful.

3.3 TOKAMAK SIZE-COST TRADE-OFFS

Extensive parametric sizing studies were not included in previous hybrid reactor efforts. The specific nature of these conceptual design studies combined with the time consuming analyses required to evaluate the alternatives did not lend itself to application of parametric trade-offs within the scope of work.

TABLE 3-3

COMPARISON OF REPRESENTATIVE PARAMETERS
FOR FOUR TNS POINT DESIGNS [2]

	TNS-1	TNS-3	TNS-4	TNS-5
TF Coil Conductor	Cu	NbTi	Nb_3Sn	Cu/NbTi
Plasma Minor Radius, a (m)	1.0	1.2	1.2	1.0
Plasma Major Radius, R (m)	4.0	5.7	5.0	4.5
Plasma Elongation, δ (-)	1.6	1.6	1.6	1.6
Aspect Ratio, A (-)	4.0	4.7	4.2	4.5
Field at TF Coil, B_m (T)	10.4	9.9	10.9	9.7
Field on Axis, B_t (T)	5.8	5.3	5.3	5.8
Toroidal Beta, β_t (%)	5.0	5.0	5.0	5.0
Plasma Current, I_p (MA)	4.1	3.8	4.3	3.6
Mean Electron Density, $\bar{n}_e$ (m^{-3})	1.6×10^{20}	1.3×10^{20}	1.3×10^{20}	1.6×10^{20}
Mean Ion Temperature, $\bar{T}_i$ (keV)	13	13	13	13
Energy Confinement Time, τ_E (s)	1.5	1.8	1.8	1.5
$\bar{n}_e \tau_E$ (m^{-3} s)	2.4×10^{20}	2.4×10^{20}	2.4×10^{20}	2.4×10^{20}
Total Volt-Seconds	41.0	55.2	51.6	43.5
Plasma Volume, V_p (m^3)	126.3	259.2	227.6	142.1
Neutron Wall Load (MW/m^2) (MW/m^2)	1.50	1.28	1.28	1.50
Total Fusion Power (MW)	558	795	698	628
Fusion Power Density (MW/m^3)	3.7	2.6	2.6	3.7
Neutral Beam Power (MW)	40	57	50	45
Steady State Burn Time (s)	16	16	16	16
Time Between Pulses (s)	300	300	300	300
TF Coil Vertical Bore (m)	6.1	7.4	7.6	9.5
TF Coil Horizontal Bore (m)	3.8	5.1	4.9	5.7
Plasma Energy/Energy Consumed	0.32	0.85	1.57	0.51
Number of TF Coils	20	20	20	20
Cost, Building & Equipment (M$)	289	434	388	436
Relative Cost	1.0	1.50	1.34	1.51
Annual Utility Cost (M$)	4.1	3.0	2.0	3.4

During the TNS (The Next Step) trade studies recently performed at Westinghouse for ORNL, a computer code, COAST was developed to perform COsting And Sizing of Tokamaks. The code was written to conduct detailed analyses of the engineering features of the next tokamak fusion device following TFTR. The ORNL/Westinghosue study of TNS involved the investigation of a number of device options, each over a wide range of plasma sizes. A generalized description of TNS was incorporated in the code and included refined modeling of over forty systems and subsystems. Considerable detailed design and analyses provided the basis for the thermal, electrical, mechanical, nuclear, chemical, vacuum and facility engineering of the various subsystems. The code provided a tool for the systematic comparison of four toroidal field (TF) coil technologies, allowing both D-shaped and circular coils. The coil technologies were: 1) copper (both room temperature and liquid-nitrogen cooled), 2) superconducting NbTi, 3) superconducting Nb_3Sn, and 4) a Cu/NbTi hybrid. For the poloidal field (PF) coil systems copper conductors were assumed. The ohmic heating (OH) coils were located within the machine bore and used an air core, while the shaping field (SF) coils were located either within or outside the TF coils. The PF coil self and mutual inductances were calculated from the geometry, and the PF coil power supplies were modeled to account for time-dependent profiles for voltages and currents as governed by input data. Plasma heating was assumed to be by neutral beams, and impurity control was either passive or by a simplified poloidal divertor system. The size modeling allowed considerable freedom in specifying physics assumptions, operating scenarios, TF operating margin, and component geometric and performance parameters. Cost relationships were developed for both plant and capital equipment and for annual utility and plasma fuel expenses. The code was used successfully to reproduce the sizing and cost of TFTR in order to calibrate the various models. The four resulting ignition tokamak parameters are shown in Table 3-3.

The COAST code does not include a representation of several features inherent in the hybrid reactors previously studies by Westinghouse. These features include the fissionable blanket, the tritium breeding blanket, superconducting poloidal field coils, variable PF coil locations outside the TF coils, complex divertor systems, thermal power conversion systems, and fuel cycle or refueling scenarios. Modifications to the COAST code to include many of these features is presently underway.

Although the analyses performed by this code are dependent on the accuracy and level of detail provided by the input and costing models, it does provide a rapid, relative comparison of design alternatives and therefore, is an excellent tool for trade studies.

3.4 CAPITAL COST ANALYSES

Most capital cost analyses have been following the format established by NUS-531 in 1969. However, a considerable difference in capital costs can result from the conservatism of the cost estimates, the contingencies assumed on individual components, and the design detail on which the cost estimate is based. For the Actinide Burner Design Study[3], contingencies on individual components as well as on the overall systems resulted in an estimated average total contingencies for first-of-a-kind components of at least 2. In the TCT Hybrid Design Study[4], the similar contingency is estimated to be about 1.5. A comparison of costs of the TCT hybrid components with the LLL mirror hybrid conducted during the same study[4] indicated considerable costing differences for similar components. Cursory comparisons with UWMAK II component costs were also made and significant discrepancies were noted. Battelle Northwest is preparing for DOE a set of guidelines for costing fusion reactor designs which includes a general approach and account numbers similar to NUS-531. However, it does not, as of yet, give unit costs such as $/kg for fabricated stainless steel or similar values which would provide a uniform cost estimating basis for preliminary conceptual designs. It is concluded that meaningful capital cost comparisons between various studies cannot be made until a uniform sizing and costing methodology is developed for hybrids which includes documented costing schemes and uniform unit costs.

3.5 SYSTEM RELATED COST IMPROVEMENTS

Another method of reducing costs in tokamak hybrid reactors is to evaluate trade-offs between two independent systems. An example of such a study was made between the PF coil system and the neutral beam injection system on the TCT Hybrid Design Concept[4]. A summary of the study results follows.

In the TCT Hybrid Breeder design the neutral beams are injected at the horizontal midplane. For reasons of refueling accessibility, it was proposed to evaluate

injection of the neutral beams nearly vertically. The horizontal midplane then becomes available as a coil location for the poloidal field coils. The extra flexibility in poloidal field coil location was explored in a limited computational study.

Design parameters shown in Table 3-4 for two poloidal field coil designs were generated and the cost difference estimated. The volume of conductor for the PF coil set design with near-vertical beam injection (the alternate) is about 28% less than that for the PF coil set corresponding to horizontal beam injection (the reference). The stored energy is about 27% less. The cost of the alternate PF coil set design, taking into account net deletion of 8 OH and 2 SF coil positions and reduction in power supplies, is about $60 M less than the reference design. Trade off studies of this nature may also be expanded by using the COAST Code to enable a better overview of the economic trade-offs. Future efforts of this type will require interactive design and COAST modeling to adequately represent the impact of design options.

TABLE 3-4

Design Parameters of Reference and Alternate
Poloidal Field Coil Sets

	Reference[1]	Alternate[2]
Amp-turns[3] - OH (MAT)	21.8	16.9
Amp-turns[3] - SF (MAT)	44.3	24.1
Amp-turns[3] - OH and SF (MAT)	66.1	41.0
Conductor Volume[3] - OH (m^3)	3.6	2.9
Conductor Volume[3] - SF (m^3)	27.0	19.1
Conductor Volume[3] - OH and SF (m^3)	30.6	22.0
Stored Energy - OH (MJ)	256	203
Stored Energy - SF (MJ)	4240	3070
Stored Energy - OH and SF (MJ)	4496	3273
Peak Vertical Force (MN)	95[4]	93[5]
Peak Radial Force (MN)	323[6]	209[7]

---

(1) Outermost PF coil must avoid neutral beam duct at horizontal midplane.

(2) PF coil allowed near horizontal midplane.

(3) Upper half plane only; double for total in coil set.
Volumes include void fraction (about 35%).

(4) At r = 6.65 m, z = 6.0 m, MAT = 2.25

(5) At r = 9.2 m, z = 2.45 m, MAT = 2.04

(6) At r = 2.95 m, z = 7.15 m, MAT = 8

(7) At r = 5.1 m, z = 6.8 m, AT = MAT = 4.4

4.0 BUNDLE DIVERTOR CONCEPT AND ANALYSIS

The application of a bundle divertor design to a tokamak hybrid reactor could lead to significant cost reductions by reducing the height of the toroidal field coils. This assumes that the concept was using a poloidal divertor above and below the plasma. The bundle divertor leads the diverted flux through an opening between two adjacent toroidal field (TF) coils to the outside of the TF coil array where the flux is expanded in both horizontal and vertical directions. The particle collection can then be handled completely outside the torus. This concept requires ingenuity to keep the inter-coil forces manageable, the conductor density acceptability low, and the shielding space between the plasma and coils adequate.

4.1 INTRODUCTION

The bundle divertor concept was evaluated in the TCT Hybrid Study[4] and considered as an alternative method for TNS[5] to replace the compact poloidal divertor. Since the physical dimensions and toroidal field intensity for a tokamak hybrid are similar to the values for these concepts, the results and arguments can apply directly to this hybrid study.

Since the current needed in the bundle divertor coils is proportional to the toroidal field and only a small bundle of toroidal flux is diverted[6], the divertor current is large, its interaction with toroidal field is strong,and particle collection surface area is small. The main advantage of the bundle divertor is that the diverted flux can be led to the outside of the TF coil array through a comparatively small aperture in the vacuum vessel. The design must accomplish this purpose with as little perturbation as possible on the rest of the system. The particular design discussed in this report is the result of examining many cases and it achieves the purposes just mentioned. A beneficial result of this particular design is that there is no torque on the coils. The current is still large and the space available for shielding must be increased. The design can be optimized to a limited extent with the electromagnetic divertor.

4.2 RESULTS

The overall design configuration was shown in Figure 2-1. The key parameters used for the calculation are B_T = 4.0 T on axis at R_o = 5.0 m and minor radius a = 1.25 m. There are 16 TF coils. The divertor consists of 5 coils and the currents carried by them are shown in Figure 4-1. The coils can be circular or rectangular; however, the latter is preferred. The center legs indicated by dots are on the axis passing through the middle of the TF coil gap; the outer leg is distributed around the TF coils. Many other designs have been evaluated and one of them is shown in Figure 4-2. The design shown in Figure 4-1 is the best in the sense that it produces a more desirable flux pattern in terms of space between the null point and the conductor, the expansion of flux, and the force distribution.

The most critical part of the bundle divertor as determined by results of this design is the center leg of the coil which carries the current I_1. The maximum field in this region calculated by a filamentary model is 6 T. The maximum current density of Nb_3Sn superconductor at 2 K is estimated to be 10 x 10^5 amp/cm^2. This is an extrapolation shown by * in Figure 4-3 by using a conductor to copper and helium cooling ratio of 60. The current density at the point shown by the circle can be used if the conductor to copper and helium cooling ratio of 40 can be used. Assuming a factor of 60 reduction in current density to provide the area required to copper stabilizer and helium cooling,[7] the overall current density is 1.66 x 10^4 amp/cm^2. Using such an extremely optimistic value, the conductor area will be 420 cm^2. The length of the center leg of the coil carrying I_1 is 60 cm. Then the width is 7 cm. Thus, the space for shielding at the minimum point is 23 cm. With some optimization, a 50 cm of shielding space is possible. The net force on this particular coil is outward and estimated to be 25 Meganewtons. A force of this magnitude can be adequately restrained.

Since the preceding analysis greatly exceeds the design goal of 4 kA/cm^2 for the current density, alternate concepts which accomplish this were evaluated. The auxiliary divertor coils shown in Figure 2-1 represents such a concept which appears to offer the potential of greatly reduced current densities.

The toroidal fluxes without divertor are shown in Figure 4-4. The projection of the lines of force produced by the divertor coil on the midplane is shown in

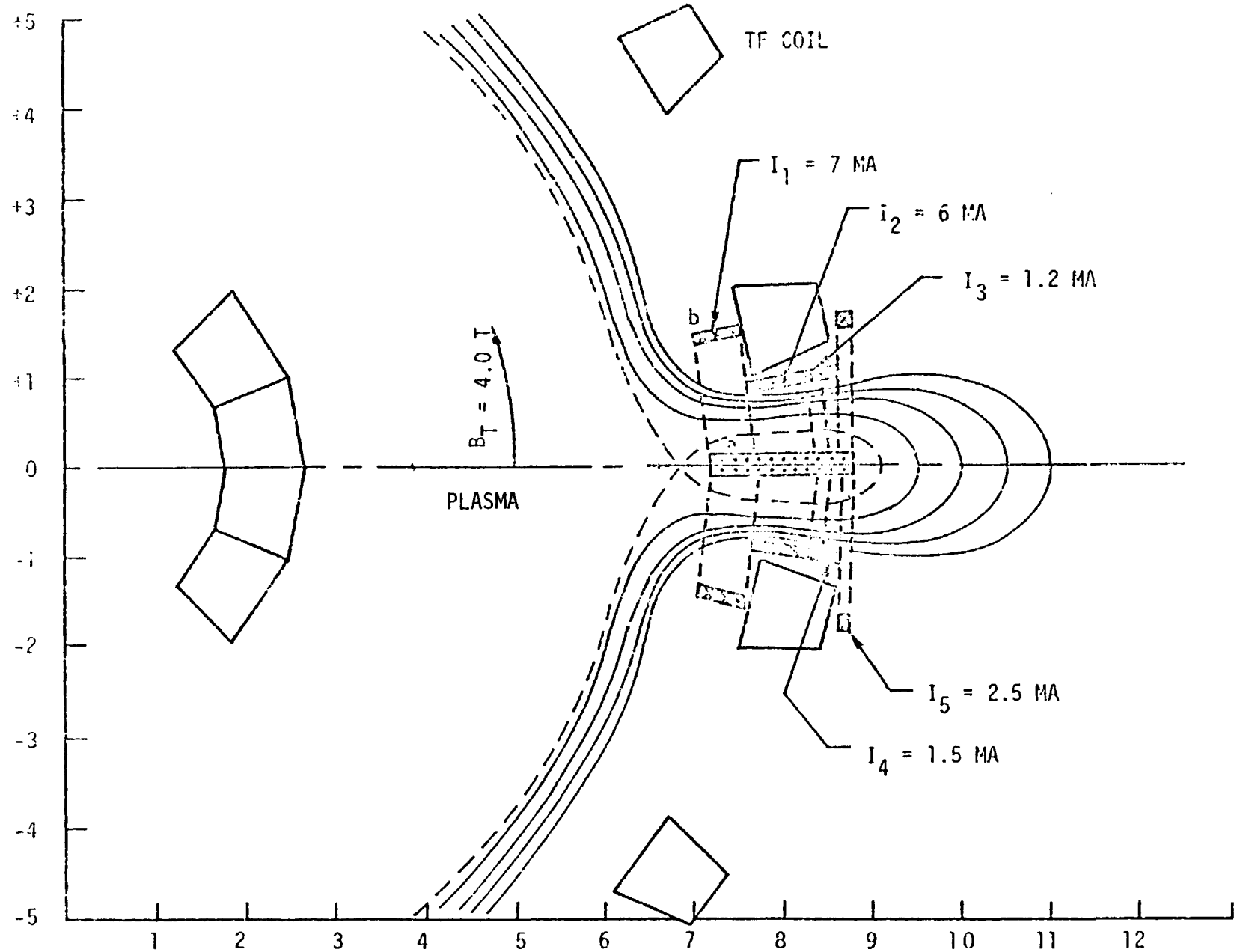

Figure 4-1. The Magnetic Flux Pattern of a Bundle Divertor Design

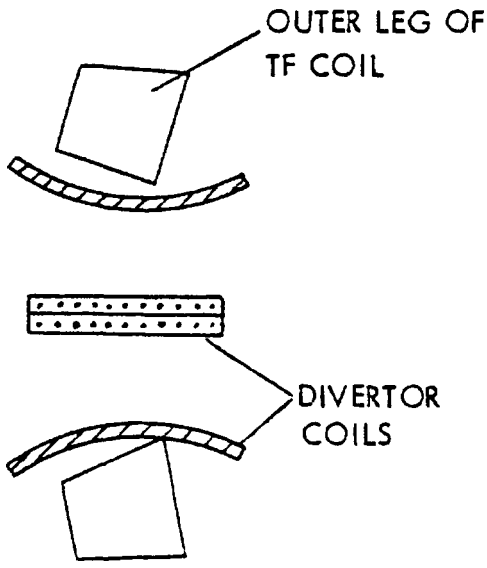

Figure 4-2. Alternative Divertor Coil Arrangement

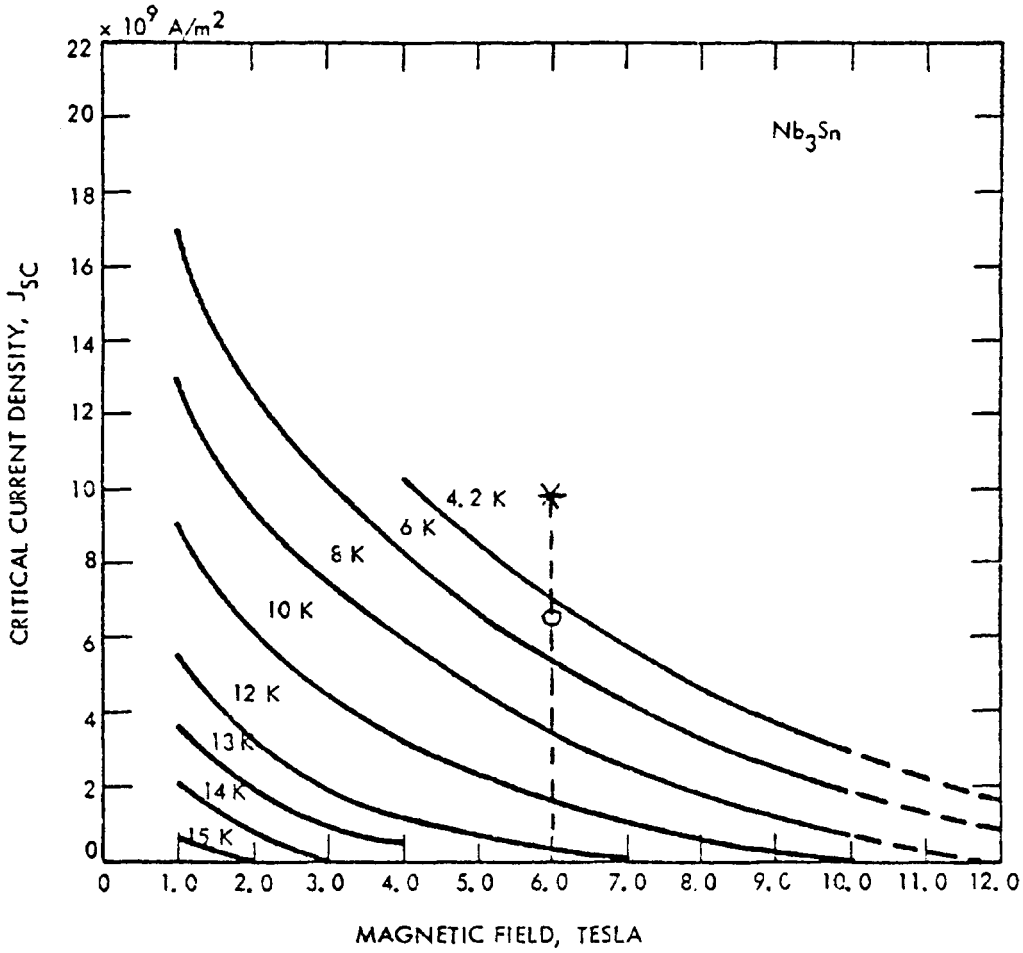

Figure 4-3. J_{sc}-H-T Diagram of Nb_3Sn Superconductor

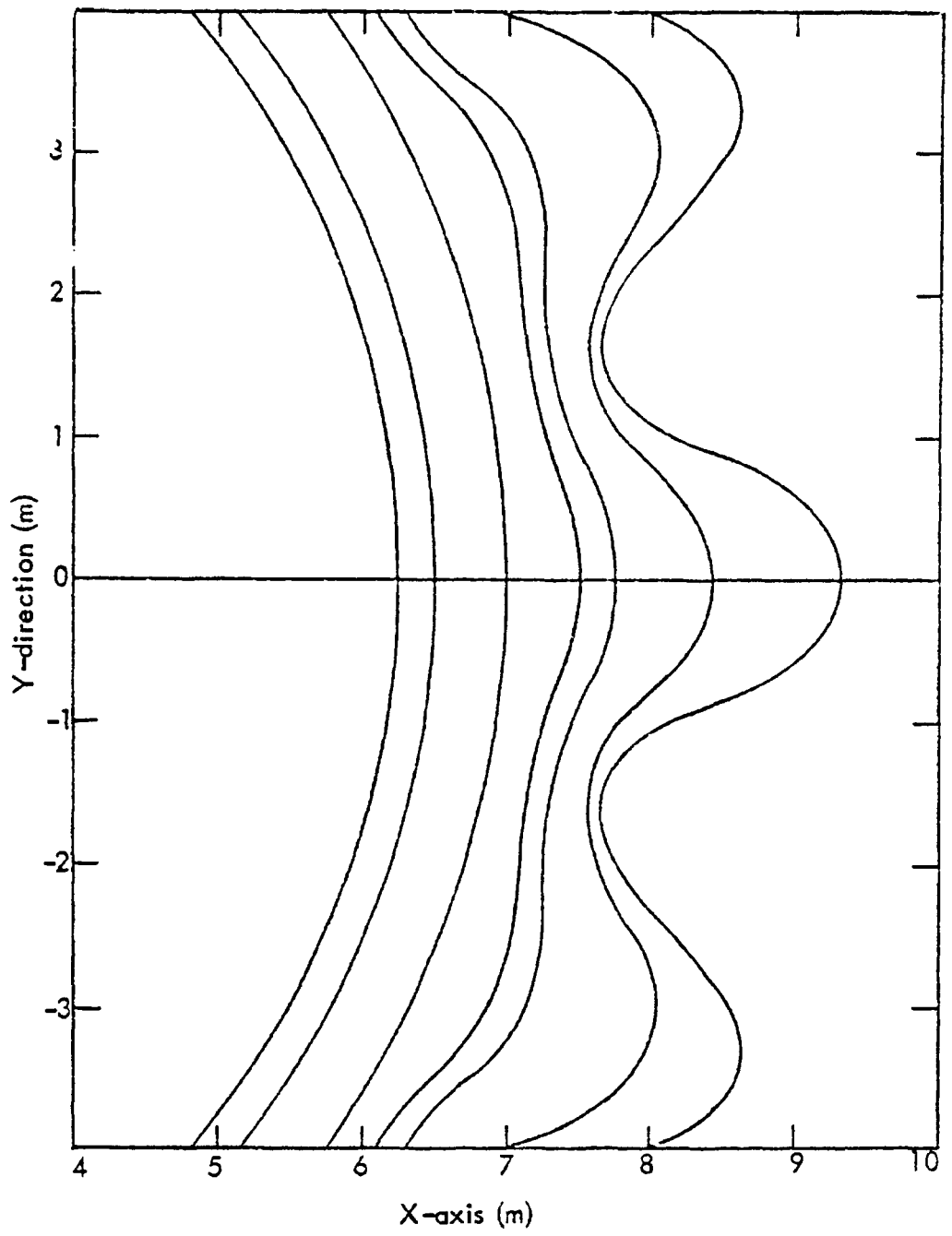

Figure 4-4. Projection of Vacuum Toroidal Field on X-Y Plane Without Divertor

Figure 4-5. The variations of the field intensities along the centerline of the gap are shown in Figure 4-6. The toroidal field changes slowly, but the divertor field falls off exponentially from the center leg of the divertor coil, where B_T is the toroidal field due to the TF coils, B_D is the field due to divertor coils alone and B is the total field. This means that an extraordinarily large current is required to move the null point further away from the conductor to increase the space between them. This in turn will increase the conductor area which is undesirable. Increasing this critical shielding space requires a larger gap instead of reducing the gap. Possible ways of improving the design are discussed as follows:

(1) Reducing the number of TF coils. This increases the ripple which causes the loss of energetic alpha particles[8].

(2) Removing one TF coil. The same purpose can also be accomplished by pushing the two adjacent TF coils apart or reducing the currents in the two adjacent coils so that they can be made narrower. The amount of current reduced can be redistributed to the other TF coils. The dominating affect may be the loss of energetic particles which causes the loss of α heating power. A preliminary analysis is as follows:

Figure 4-6 shows the total field, $B_\phi(R)$, curve as determined from $B_T(R) - B_D(R)$. The ripple at the plasma surface for R = 6.25 m is

$$\text{Ripple} = \frac{B_T(R) - B_\phi(R)}{B_T(R)} \times 100 = \sim 30\%$$

This ripple is localized and the loss may be small although the ripple is large. To see this, a sketch of the magnetic field intensity along a field line and the trapping region on a r-Θ plane is shown in Figure 4-7. Assuming q = 2.5, the angular limits of the ripple are approximately

$$-\phi_1 = \phi_2 = \frac{360}{Nq} = 22\frac{1}{2}^\circ \qquad (1)$$

where N = 16 is the number of TF coils. The ripple can roughly be represented by

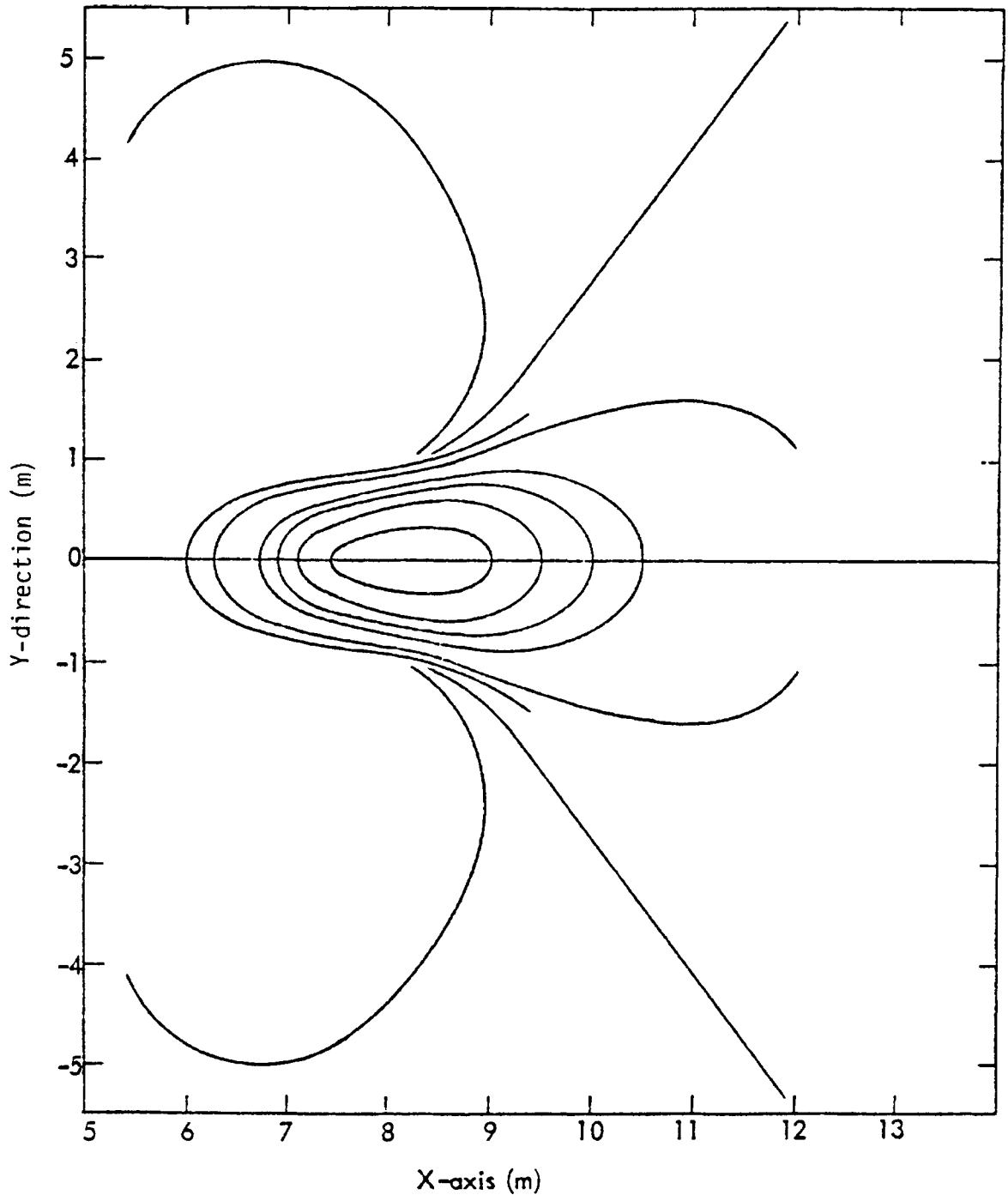

Figure 4-5. Projection of Vacuum Field on X-Y Plane Produced by Divertor Coils

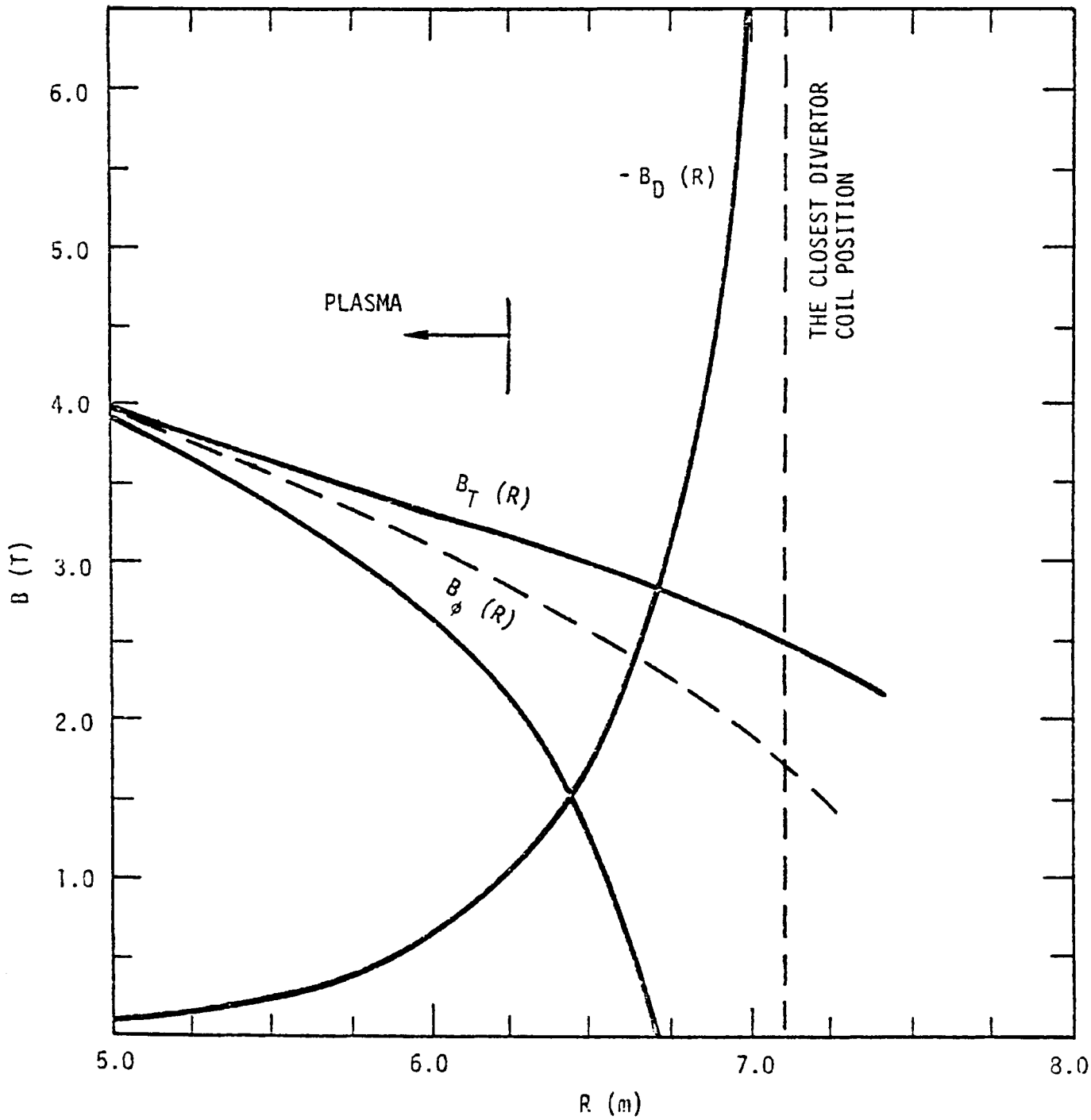

Figure 4-6. Variations of Field Intensity Along The Centerline of the Divertor

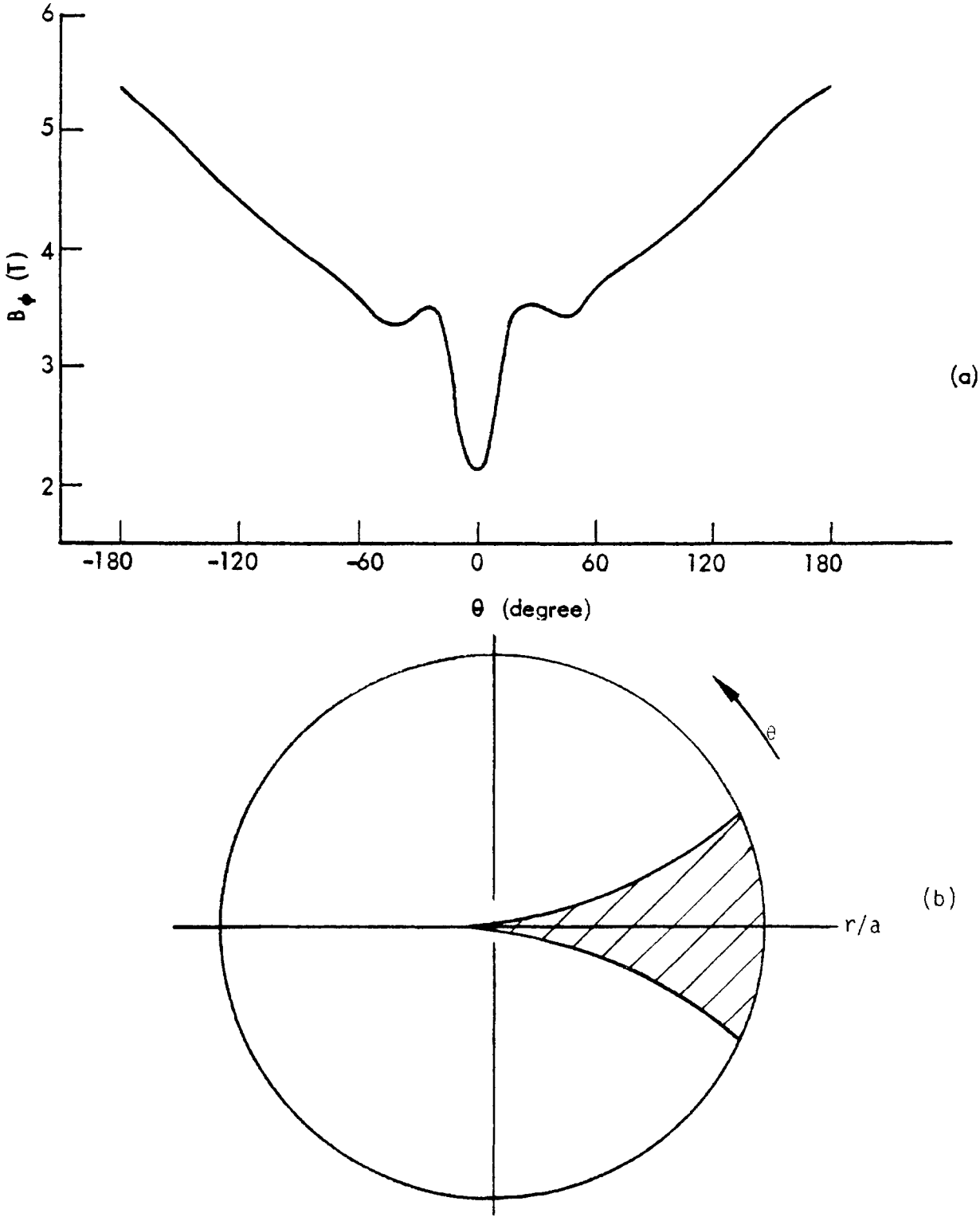

Figure 4-7. Localized Field Ripples Produced by Bundle Divertor
(a) Magnetic Field Along a Line of Force
(b) Schematic Picture of Particle Trapping Region (Shaded Area) on r-θ Plane

$$\xi(r,\theta) = \xi_a \left(\frac{r}{a}\right)^n \exp\left(-\left(\frac{\alpha\theta}{\pi}\right)^2\right) \tag{2}$$

where ξ_a is the ripple at r = a, θ = o, n = 2 and α = 3. The total field can be written as follows if $\phi_1 < \phi < \phi_2$:

$$B_\phi(r,\theta,\phi) = \frac{B_t}{1 + \frac{r}{R}\cos\theta}\,[1 - \xi(r,\theta)\cos(N\phi)], \tag{3a}$$

if $\phi < \phi_1$ or $\phi > \phi_2$ the total field equation is

$$B_\phi(r,\theta,\phi) = \frac{B_t}{1 + \frac{r}{R}\cos\theta} \tag{3b}$$

where B_t is the plasma field on axis.

The fraction of energetic particles trapped in the ripple can be written as

$$f_T = \frac{\sqrt{\xi_a}\int_{\phi_1}^{\phi_2}\sqrt{1-\cos\phi}\,d\phi\int_0^a rdrS(r)\left(\frac{r}{a}\right)^2\int_0^\pi \exp\left(-\frac{1}{2}\left(\frac{\alpha\theta}{\pi}\right)^2\right)d\theta}{2\pi^2\int_0^a rdrS(r)} \tag{4}$$

where S(r) is the source function and is taken to be a parabolic function of r. Then, f_T can be approximated as

$$f_T \cong \frac{\sqrt{2\pi}}{5Nq}\sqrt{\xi_a} \leq 0.05\%. \tag{5}$$

The toroidal field required to move the null point away from the conductor by 10 cm can be predicted and is shown by the dashed curve in Figure 4-6. This increases the ripple by 1%. The total ripple is still only 31%. Therefore, the effect of this kind of localized ripple in terms of the loss of energetic α particles is not significant. The effect on MHD equilibria, stability and particle transport has to be evaluated. The effect on the mechanical structure of the TF coil array has to be carefully analyzed.

(3) Reducing the toroidal field. To gain 10 cm in space B_o has to be reduced to 3.5 T.

(4) Using an electromagnetic divertor[9]. The thermal velocity of the plasma streaming through the divertor throat is

$$V = 9.79 \times 10^3 \sqrt{T_i/\mu_i} \quad (m/sec), \tag{6}$$

where μ_i is the mass ratio of the charged particle and proton, and T_i is in eV. For T_i = 1 keV and using the mass of tritium

$$V \cong 1.8 \times 10^5 \text{ m/sec.} \tag{7}$$

The magnetic field near the separatrix and null point is less than 0.2 T. Then the electric field required to produce a perpendicular drift at the same velocity is

$$E = B \times v = 2.6 \text{ keV/m} \tag{8}$$

by assuming that the plasma is in contact with the electrode[10]. Such a system is illustrated in Figure 4-8a. The resultant separatrix is illustrated by the broken curve of Figure 4-8b. The plasma shielding effect and damage to the electrodes have to be studied. The probability of developing a practical bundle divertor will be much improved if this method is feasible.

4.3 PARTICLE COLLECTION SCHEMES

A brief evaluation of an alternate direct energy conversion method is discussed which differs from the frequently mentioned schemes such as liquid lithium, the moving metal belt and supersonic jet stream. The direct energy conversion methods for mirror and tokamak have been discussed in detail by Moir[11]. It is not practical for energy recovery in this case because the flux expansion is not as good as Moir assumed. The main purpose here is to use the method to slow down the particles so that they will land softly on the collector. This will make the collector design simpler and heat dissipation less. A simple design is illustrated in Figure 4-9. The average mirror ratio, B_m/B of the fields at mid-point of the divertor throat, B_m, and at the collectors, B, is about 10, so that the perpendicular energy near the collector is

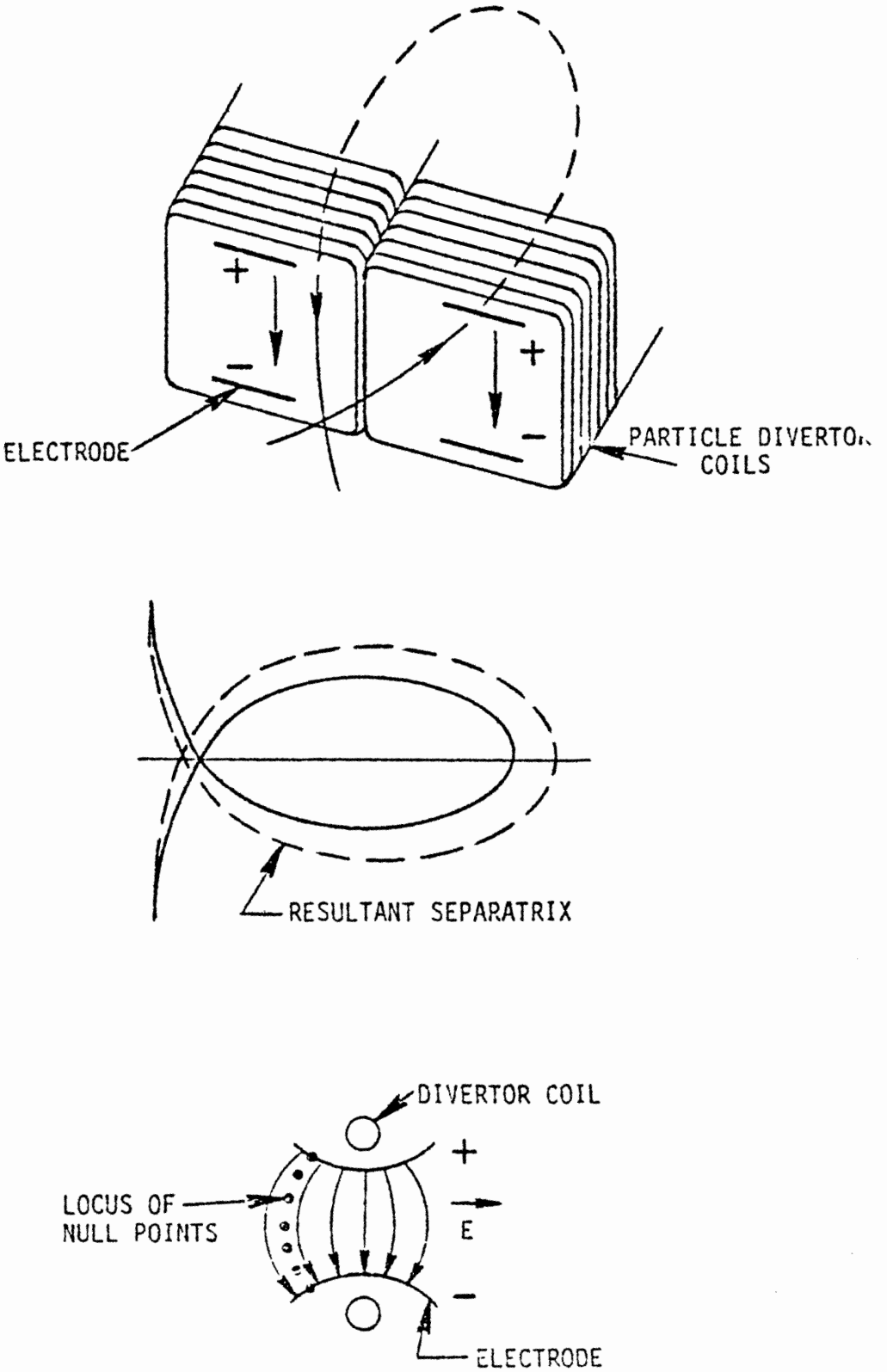

Figure 4-8. Electromagnetic Bundle Divertor

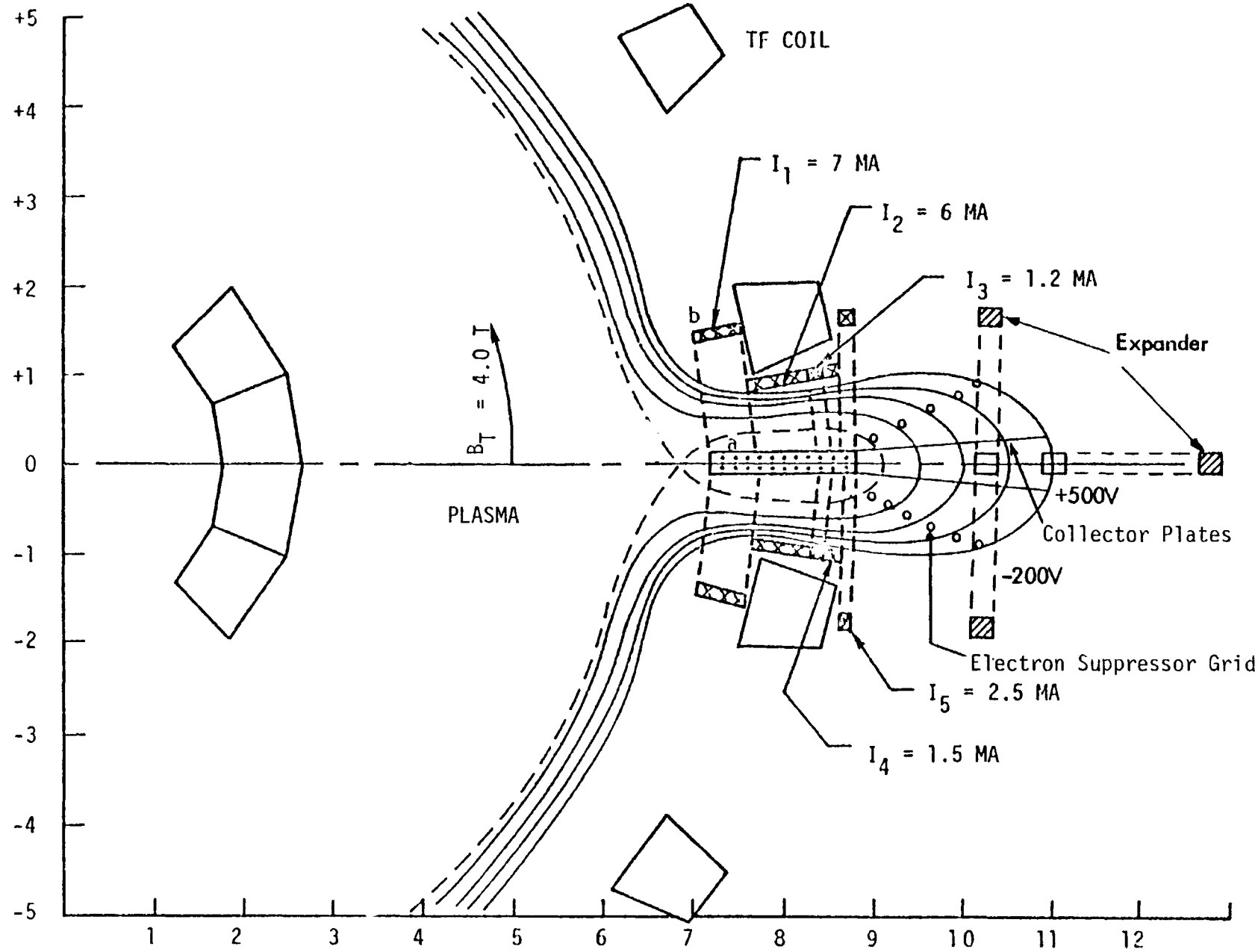

Figure 4-9. Illustration of the Direct Conversion Scheme for Particle Collection

$$W_{\perp} = W_{\perp M} \frac{B}{B_m} = 0.1 \text{ keV}. \quad (9)$$

Then the parallel energy is 0.9 keV, so that the voltage on the collector plate can be set at 0.5 keV to slow down the particles. The energy recovery efficiency may be about 30%. The negative grids, which are used to repel the electrons, may impose a problem because the heat dissipating on them is very high. The fluxes can be further expanded by the additional coils shown in Figure 4-9 (expander coils).

4.4 CONCLUSIONS

A bundle divertor concept has been developed which will lead the diverted flux to the outside of the TF coil array. The forces are reduced to a manageable level. The fluxes are expanded so that workable particle collection methods, such as direct energy conversion schemes, can be employed. An electromagnetic bundle divertor is proposed to enlarge the space enclosed by the loop of the separatrix. Provision for 50 cm of shielding and structure space may be possible with a combination of the modifications suggested and assuming very optimistic current density of Nb_3Sn at 2 K. This system is worthwhile for further study if adequate shielding can be provided and the technological feasibility of using the auxiliary divertor coils to reduce the superconductor current density to 4 kA/cm^2 can be verified. The concept shown in Figure 2-1 appears to offer a feasible approach to evaluate for achieving these goals.

5.0 THORIUM FUEL CYCLE BLANKET ANALYSES

The principal emphasis of the work in the nuclear area described here is on the preliminary selection of blanket lattice arrangements leading to high performance in ^{233}U breeding, tritium breeding and thermal power production under an assumption that the initial blanket fuels may be enriched.

5.1 BASIS FOR NEUTRONIC ANALYSES

The multi-variable design space in the blanket was evaluated using the methodology of the design of experiments, as applied to nuclear design[13]. For this purpose, central composite orthogonal designs were set up, which made it possible to examine simultaneously the effect on the breeding and energy generating performance of the blanket for changes in the values of the principal design parameters.

Using four group cross sections collapsed by ANISN from the 100-group DLC2F library from the Actinide Burner Study[3], one-dimensional FORGOD runs were set up to obtain time independent BOL power densities and T-breeding rates. Using the output power densities and lattice specifications, temperature and pressure drop calculations were set up for the HECTIC code. Using HECTIC output temperatures and pressure drops for given coolant flow rates, the energy conversion efficiencies were calculated for other Rankine or Brayton cycles.

Generation of cross sections for the present phase of nuclear design were carried out with the VITAMIN-C code system. The input to the VITAMIN-C requires specification of zonal mixes and the generation of the resultant neutron spectra. This effort was completed with the initial parametric study.

Preliminary estimates have been obtained of the neutron capture rate and the thermal power prediction in the blanket of a hybrid breeder reactor at beginning of life conditions.

A reactor with a fissile breeding blanket placed on the outside of the plasma region was assumed with the tokamak geometry identical to that used for the Pu-U hybrid breeder[4]. The differences from the Pu breeder are:

- Neutron wall loading was increased to 4 MW/m^2
- The same blanket width was initially divided into 3 zones: the fast neutron multiplier zone loaded with U+Pu; the Th containing breeding zone; and the Li_2O containing T-breeding zone.

The initial calculations used a carbide form of fuel in TZM cladding in the Th-containing region. Helium cooling was assumed. A mix of natural UC with PuC to provide a range of fissile enrichments was used for the neutron multiplier zone, with appropriate fuel rod diameter and pitch to handle the higher power densities expected. Replacement of U by Th in the multiplier zone was considered.

The combined width of the first two zones was initially fixed at 50 cm and 20 cm was allotted to the Li containing zone. Natural Li was specified for that zone. The entire width of the 70 cm loading zone was assumed to be traversed by the fuel rods pointing one end towards the plasma. The dimensions of the rods and their spacing, i.e. the lattice description, is given in Table 5-1. The initial blanket model for the one-dimensional calculation of neutron distribution and power is given in Table 5-2. Subsequent changes were made to this model in the fuel zones (11, 12 and 13) as defined in the respective tables. The schematic top view of a reactor segment is shown in Figure 5-1. The number densities of constituents of the blanket are given in Table 5-3.

The calculations were set up in conformity with two variables: the atom percent of Pu in a U plus Pu carbide mix and the thickness of the zone containing this material. The Pu composition was assumed to consist of 69.6% ^{239}Pu and 30.4% ^{240}Pu. This approximates the composition of Pu discharged from an LWR at 33 GWd/tonne burnup, if ^{239}Pu and ^{241}Pu are lumped under ^{239}Pu, and if ^{238}Pu, ^{240}Pu, and ^{242}Pu are lumped together under ^{240}Pu.

TABLE 5-1

Lattice Specification

Carbide pellet diameter, d	=	0.75 cm
Triangular rod pitch, p	=	0.95 cm
$\frac{P}{d_{pellet}} = 1.267$		$\frac{P}{d_{clad}} = 1.12$
Volume fraction of fuel	=	0.5652
clad	=	0.1507
He coolant	=	0.2841
		1.0000
UC density (94.6% theoretical)	=	12.9 g/cc
ThC density (94.6% theoretical)	=	10.04 g/cc
Wire wrap diameter	=	0.10 cm
Clad thickness	=	0.05 cm

TABLE 5-2

INITIAL BLANKET MODEL

Zone Number	Mix Number	Mesh Pt. Number	Outer Rad. (cm)	ΔR (cm)	Material	
1	1	4	219.	219.	100 V	Center Void
2	3	17	229.	10.	40 SS, 40 B_4C, 20 V	Shield
3	4	7	239.	10.	50 Inc. 50 C	Reflector
4	20	21	269.6	30.6	100 Be	N. Multiplier-Reflector (Inner T-Breeding Zone)
5	17	8	302	32.4	100 Li	40% Enriched Li
6	7	8	329.	27.	26 SS, 74 V	Structure
7	4	2	330.	1.	100 Mo	1-st wall
8	1	2	565.	235.	100 V	Plasma
9	4	2	566.	1.	100 Mo	1-st wall
10	5	3	610.	44.	6 SS, 94 V	Structure
11	2,10,11	10	Var.	Var.	56 UPuC,* 15 MO, 28V	Neutron Multiplier
12	12	29	660.	Var.	56 ThC, 15 Mo, 28 V	Fissile Breeding Zone
13	13	10	680.	20.	56 Li_2O, 15 Mo, 28 V	Tritium Breeding Zone
14	8	15	714.	34.	42 SS, 58 V	Structure
15	18	45	747.	18.	91 Inc., 9 C	Reflector
16	3	67	787.	40.	40 SS, 40 B_4C, 20 V	Shield

*Pu content is a variable in this calculation

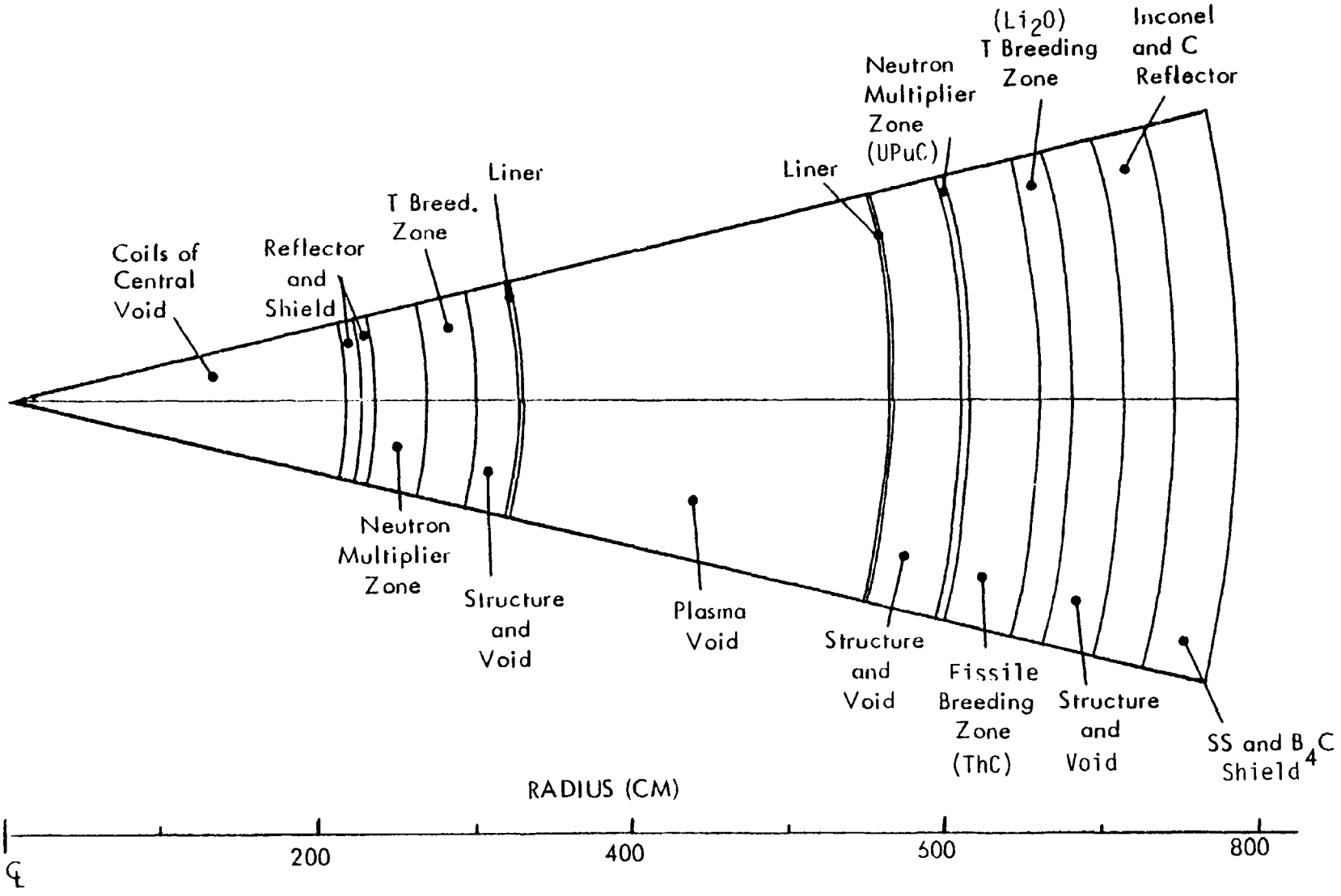

Figure 5-1. Top View of the Simplified Geometry Model Used in Scoping Calculations

TABLE 5-3

Outside Blanket

Neutron Multiplier Zone Mix Number Densities

Isotope		Mix Number		
		Number 2	Number 10	Number 11
1	^{235}U	1.246 (-4)	1.184 (-4)	1.211 (-4)
2	^{236}U	0.0	0.0	0.0
3	^{238}U	1.744 (-2)	1.657 (-2)	1.570 (-2)
4	^{239}Pu	0.0	6.066 (-4)	1.216 (-3)
5	^{240}Pu	0.0	2.650 (-4)	5.313 (-4)
6	F.P.	0.0	0.0	0.0
7	C	1.756 (-2)	1.756 (-2)	1.756 (-2)
8	Ti	9.701 (-5)	9.701 (-5)	9.701 (-5)
9	Mo	9.631 (-3)	9.631 (-3)	9.631 (-3)

Breeding Zone Mixes: ^{233}U and T

Isotope		Mix Number 12	Isotope	Mix Number 13
1	^{232}Th	1.480 (-2)	Li-6	3.469 (-3)
2	^{233}Pa	0.0	Li-7	4.241 (-2)
3	^{233}U	0.0	O	2.294 (-2)
4	^{234}U	0.0	Ti	9.701 (-5)
5	F.P.	0.0	Mo	9.631 (-3)
6	C	1.480 (-2)		
7	TI	9.701 (-5)		
8	Mo	9.631 (-3)		

The calculated power production and the ^{233}U breeding are based on the BOL absorption rate in thorium and prorated to one year of operation at 100% plant factor. The criteria for acceptable performance was established in the following manner for the fuel breeding and thermal performance.

^{233}U Production

Assume that at least 5 reactors using 180 kg/yr should be the minimum refueling goal of the hybrid. This is 1440 kg/yr based on a 75% plant availability, a 83.3% plasma duty cycle and linear performance; use 1.5 tonnes/yr as an acceptable value.

Tritium Breeding

Based on TCT Hybrid T-breeding ratio requirement of 1.17, use ∿1.2 for T-BR.

^{239}Pu Production

No net production; assume ±0.5 tonnes/year meets this goal to allow for the analysis accuracy in the scoping work.

Thermal Power Required

a) Power Plant: If a 1 GW_e power plant is desired and assuming 1 GW_e to operate the plant, 40% power conversion efficiency, an 83.3% plasma duty cycle and 75% plant availability, the thermal power at 100% plant factor is ∿8 GW_t. Use ∿8 GW_t.

b) Breakeven: Assume that a pessimistic value of <1 GW_e will operate all the plant power systems. During shutdown periods, only ∿100 MWe are required, which can be taken from a utility grid. If a power conversion efficiency of 40% is assumed then 2.5 GW_t are needed at its plant capacity factor. Assuming an 83.3% plasma duty cycle, then ∿3 GW_t at 100% plant factor is needed. Use ∿3 GW_t.

5.2 INITIAL PARAMETRIC STUDIES

The initial parametric studies are divided into four groups. Group A evaluated ^{233}U production by varying the Pu enrichment and neutron multiplier zone thickness allowing the tritium breeding and thermal power to fall out as dependent variables. These results are shown in Table 5-4 with the response surfaces

TABLE 5-4

BLANKET PARAMETRIC CALCULATIONS - GROUP A

Case No.	Blanket Zone Width, cm (a)			Pu Enrichment, a/o P_u (b)	Initial Inventory, (c) tonnes			Tritium Breeding Ratio	Fissile Production BOL-(tonnes/year)(d)		Blanket Thermal Power (BOL)(d) (GW)
	Neutron Multiplier U, PuC	Fissile Breeder ThC	Tritium Breeder Li_2O		Pu	U	Th		^{233}U	^{239}Pu	
1	2	48	20	0	0	30.2	620	0.44	3.7	0.5	1.2
2	6	44	20	0	0	91.0	570	0.46	3.2	1.5	2.0
3	10	40	20	0	0	152.1	520	0.47	2.6	2.4	2.5
4	2	48	20	5	1.5	28.7	620	0.45	3.8	0.3	1.5
5	6	44	20	5	4.6	86.4	570	0.48	3.5	1.1	2.9
6	10	40	20	5	7.6	144.5	520	0.51	3.1	1.9	4.2
7	2	48	20	10	3.0	27.2	620	0.46	4.0	0.2	1.8
8	6	44	20	10	9.1	81.9	570	0.51	3.9	0.6	4.1
9	10	40	20	10	15.2	136.9	520	0.56	3.8	1.2	6.6

(a) Zones are NM-neutron multiplier; FB - Fissile Breeding; TB - Tritium Breeding. Order listed is closest to plasma first and then outward sequence. The fusion power source density is assumed to be 4 MW/m^2 at the first wall for all cases.

(b) Pu is assumed to be 69.6% fissile from LWR discharge. The Pu enrichment is in neutron multiplier zone.

(c) This group uses TZM clad.

(d) These values are at 100% plant capacity factor.

plotted in Figures 5-2 and 5-3. The shaded area in Figure 5-3 indicates performance meeting the minimum value of the acceptance criteria previously established. The tritium breeding performance was not acceptable for any of these cases, varying from a ratio of 0.44 to 0.56 compared to the 1.2 required value. The ^{233}U production was adequate for all cases studied although it decreased as the neutron multiplier zone width was increased. The combined zone thickness being held constant at 50 cm probably caused this effect. A ^{239}Pu production of zero was not achieved, although further optimization could have accomplished this goal. The thermal power was inadequate until a Pu enrichment of 5% was used in a 10 cm zone or 10% in a 6 cm zone width. Case no. 8 appears to be the best of those studied in this set. Further parametric studies to increase tritium breeding and reduce Pu production were deemed necessary.

Group B studies concentrated on achieving acceptable tritium breeding by further increases in Pu enrichment (to 15 a/o) in the neutron multiplier zone, adding 5 a/o Pu enrichment in the thorium breeder zone, using stainless steel clad, and increasing the width of the tritium breeding zone. These results are presented in Table 5-5 and plotted in Figures 5-4, 5-5, 5-6 and 5-7. Only case 9 resulted in sufficient T-breeding although cases 6 and 8 were marginal. A design range of T-BR $\geq$ 1.0 to $\leq$1.2 is shown cross-hatched on these figures. The other design criteria are shaded in Figures 5-5, 5-6 and 5-7. The darkened area then shows the "design space" meeting the previous criteria. Figure 5-7 shows that no point design will meet all the criteria. The reduced width of the thorium breeder zone resulted in some cases of unacceptable ^{233}U production, thus indicating that a width of 5 to 10 cm is probably the minimum to consider. Pu production of 0.1 in case 9 is considered a net of zero. It was noted that Pu burnup occurred in cases 4, 7 and 8. Adequate to extremely high (25 GW) thermal power was noted. The fuel rod maximum power density was over 1000 W/cm^3 for cases 7, 8 and 9. Although this is less than the 2200 value used in FFTF, it may require further evaluation in the hybrid applications, depending on coolant choice and fuel rod design. It was concluded that although tritium and ^{233}U breeding could be adequately achieved with Pu production controlled, the high initial inventory of Pu (27 to 38 tonnes) and the high thermal power may not be compatible with the probable fuel processing and power conversion technologies of the year 2000. Alternate methods of achieving tritium breeding would be necessary for nearer term applications.

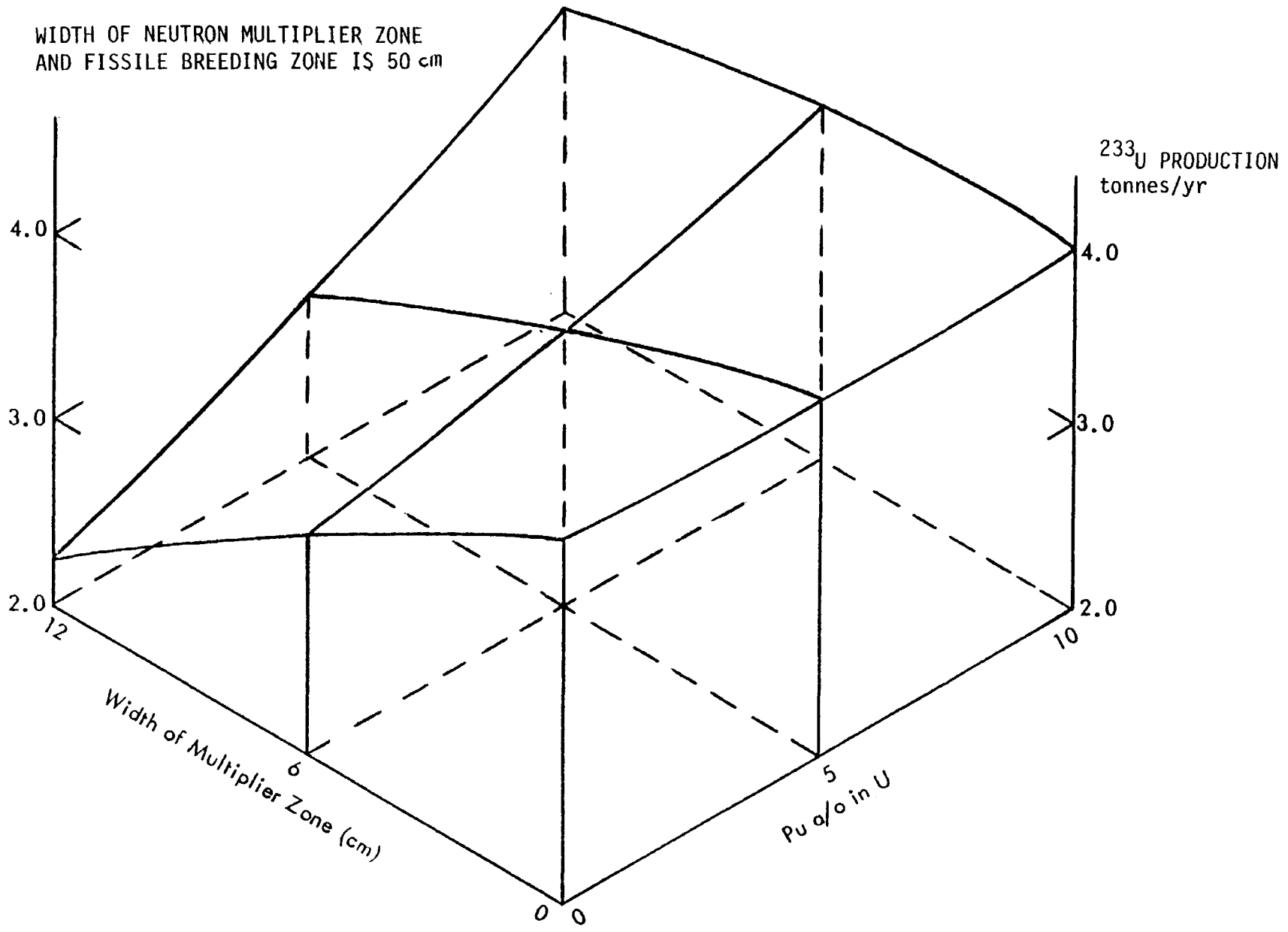

Figure 5-2. Effect of Multiplier Zone Width and Pu Content on ^{233}U Production

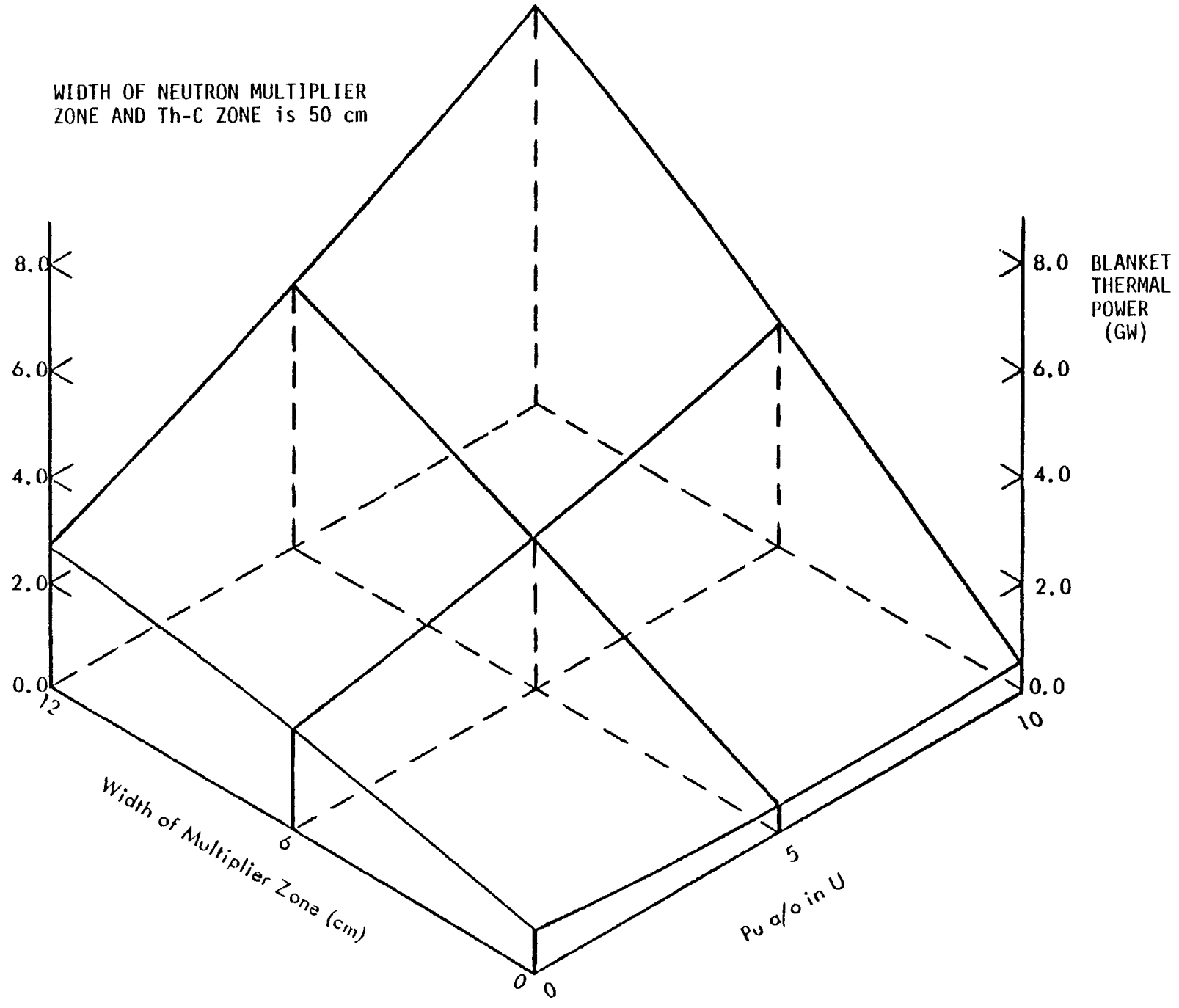

Figure 5-3. Effect of Multiplier Zone Width and Pu Content on Blanket Power

TABLE 5-5

BLANKET PARAMETRIC CALCULATIONS - GROUP B

Case No.	Blanket Zone Width, cm[a]			Pu Enrichment, a/o P_u[b]	Initial Inventory,[d] tonnes			Tritium Breeding Ratio	Fissile Production BOL (tonnes/year)[e]		Blanket Thermal Power[e] (BOL) GW	Max. Fuel Rod Power Density (W/cm^3)
	Neutron Multiplier U, PuC	Fissile Breeder Th PuC[c]	Tritium Breeder Li_2O/C		Pu	U	Th		^{233}U	^{239}Pu		
1	5	15	35/15	5	15.3	72	214	0.68	2.9	0.2	5	513
2	10	10	35/15	5	15.4	145	143	0.75	1.8	1.6	6	333
3	15	5	35/15	5	15.4	219	72	0.80	0.8	3.0	7	542
4	5	15	35/15	10	19.2	68	214	0.74	3.2	-0.3	6	735
5	10	10	35/15	10	23.0	137	143	0.88	2.2	0.8	10	816
6	15	5	35/15	10	26.9	206	72	1.03	1.1	2.0	13	882
7	5	15	35/15	15	23.0	65	214	0.81	3.5	-0.9	8	1000
8	10	10	35/15	15	30.7	130	143	1.08	2.8	-0.5	15	1232
9	15	5	35/15	15	38.4	196	72	1.50	1.7	0.1	25	1520

(a) Zones are NM-neutron multiplier; FB - Fissile Breeding; TB - Tritium Breeding. Order listed is closest to plasma first and then outward sequence. The fusion power source density is assumed to be 4 MW/m^2 at the first wall for all cases.

(b) Pu is assumed to be 69.6% fissile from LWR discharge. The Pu enrichment is in neutron multiplier zone.

(c) Pu is enriched to 5 a/o in Th, PuC.

(d) This group uses stainless steel clad in lieu of TZM.

(e) These values are at 100% plant capacity factor.

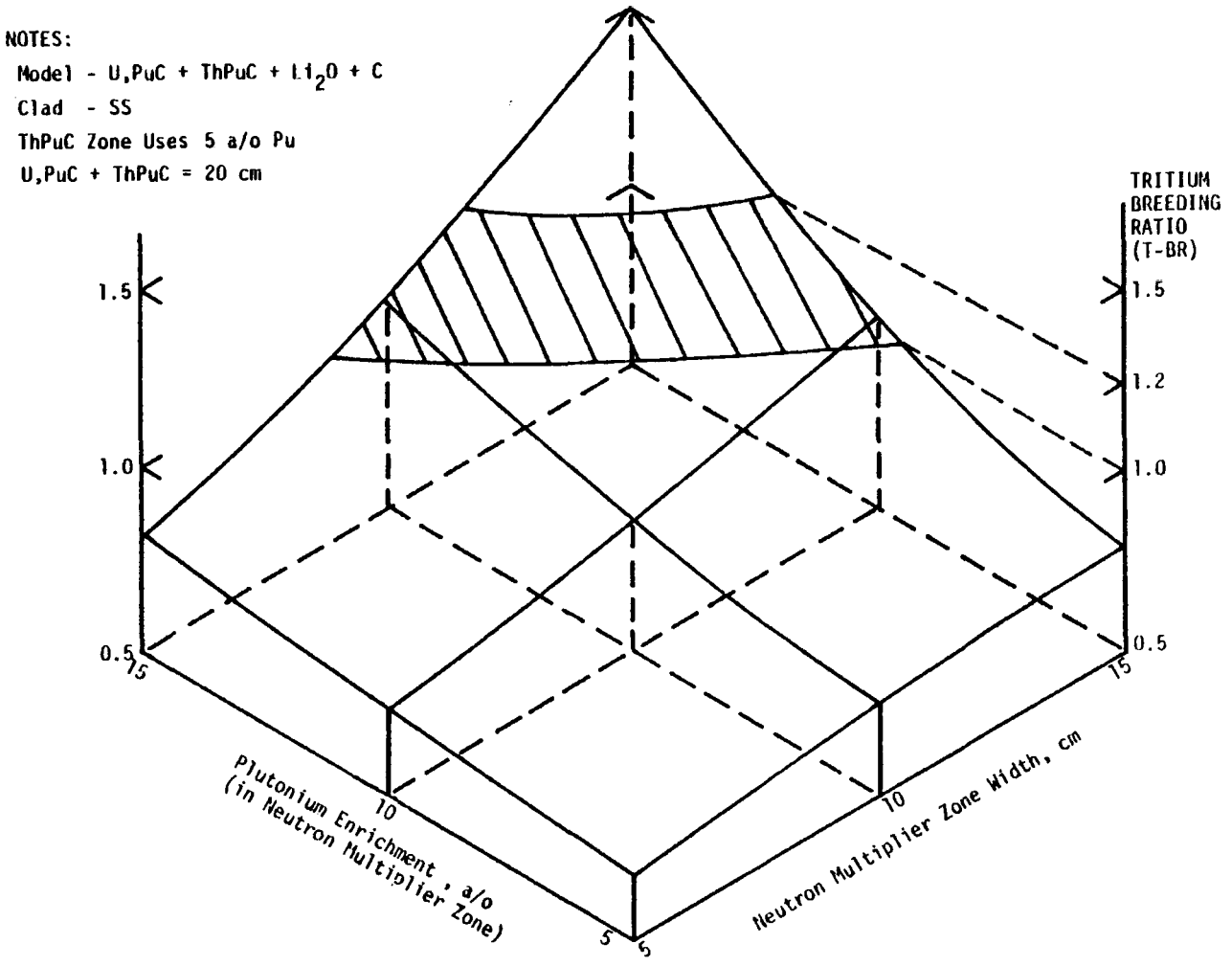

Figure 5-4. Tritium Breeding Ratio Versus Neutron Multiplier Width and Enrichment

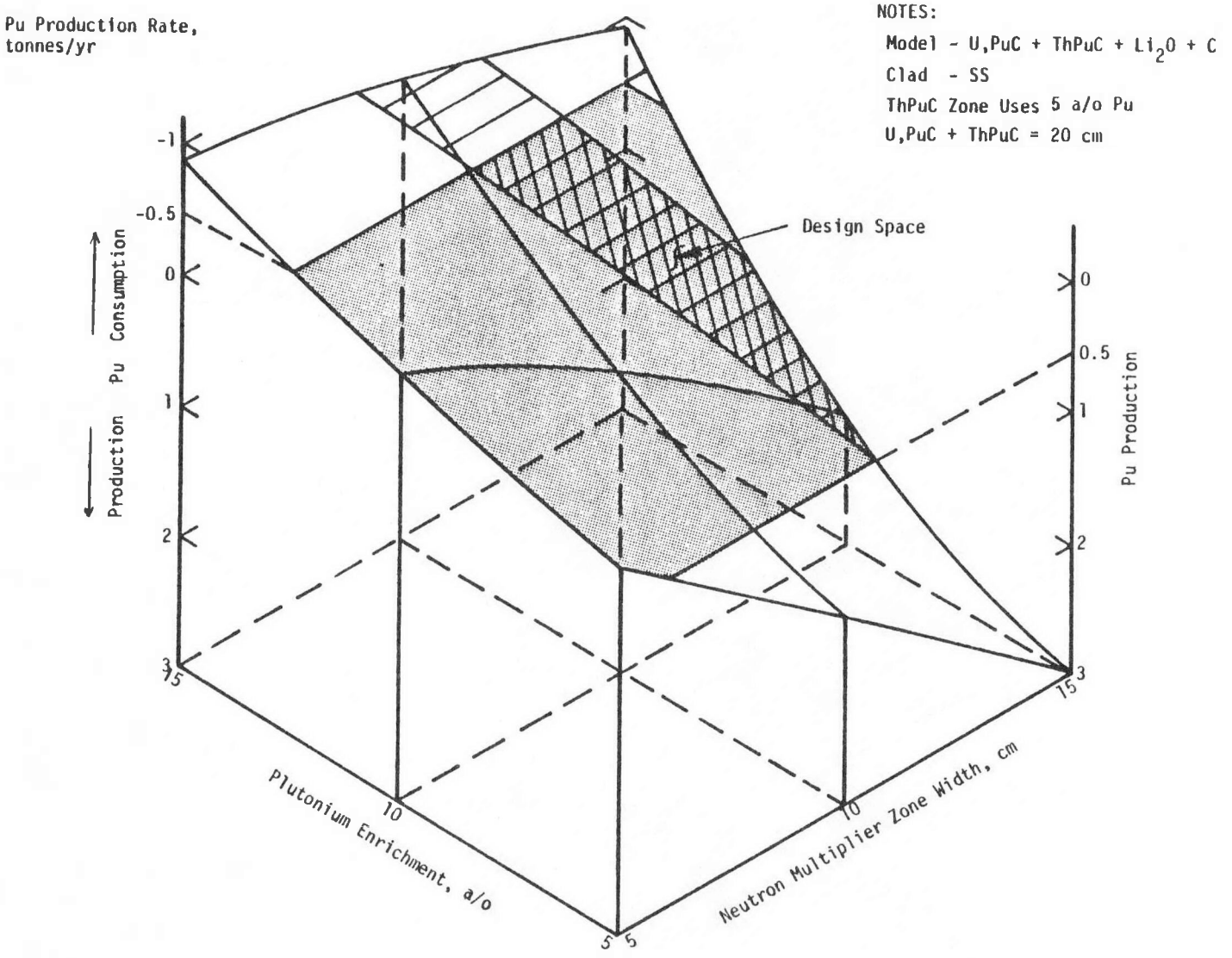

Figure 5-5. Plutonium Production Rate Versus Neutron Multiplier Zone Width and Enrichment

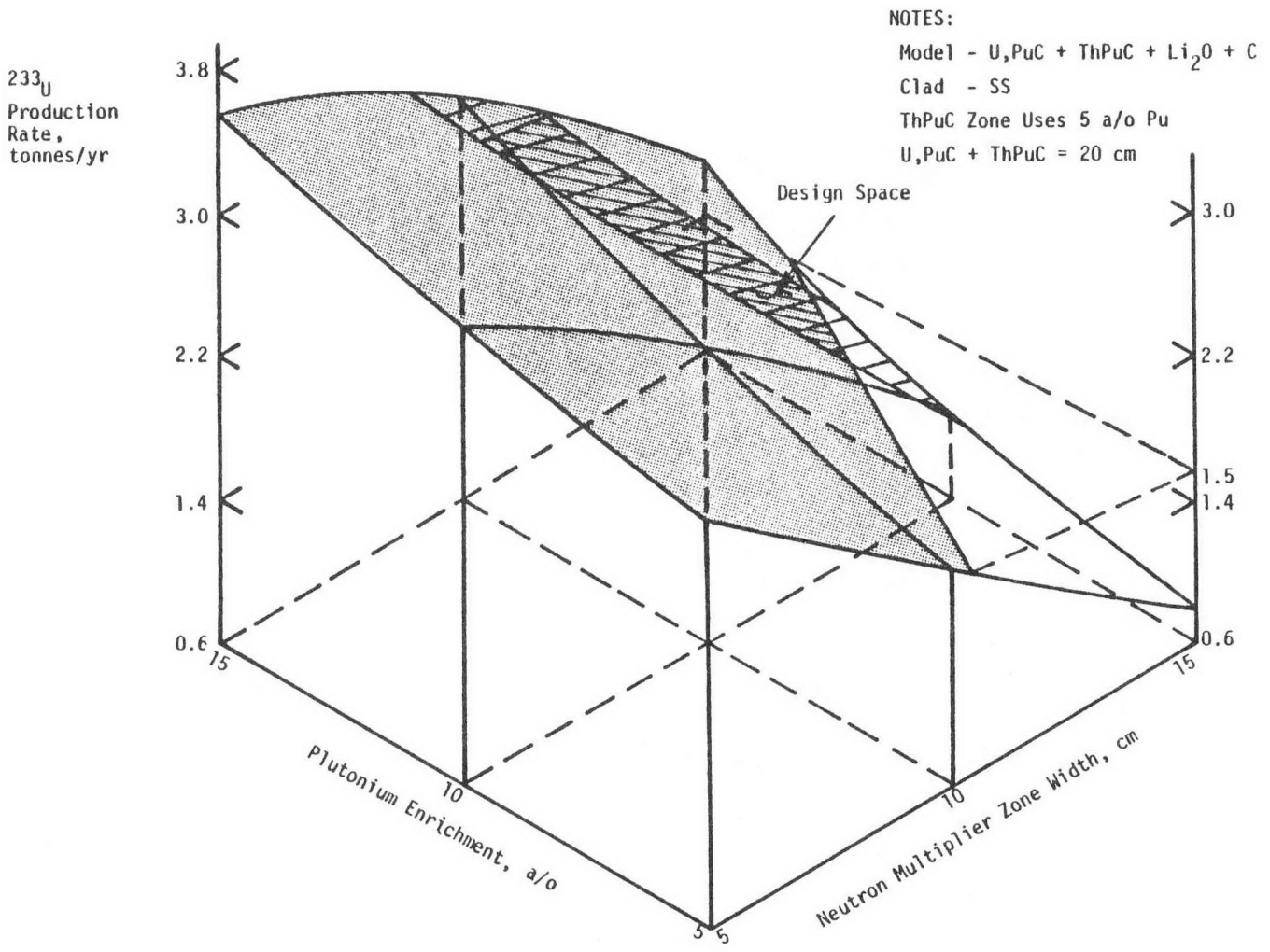

Figure 5-6. Uranium 233 Production Rate Versus Neutron Multiplier Width and Enrichment

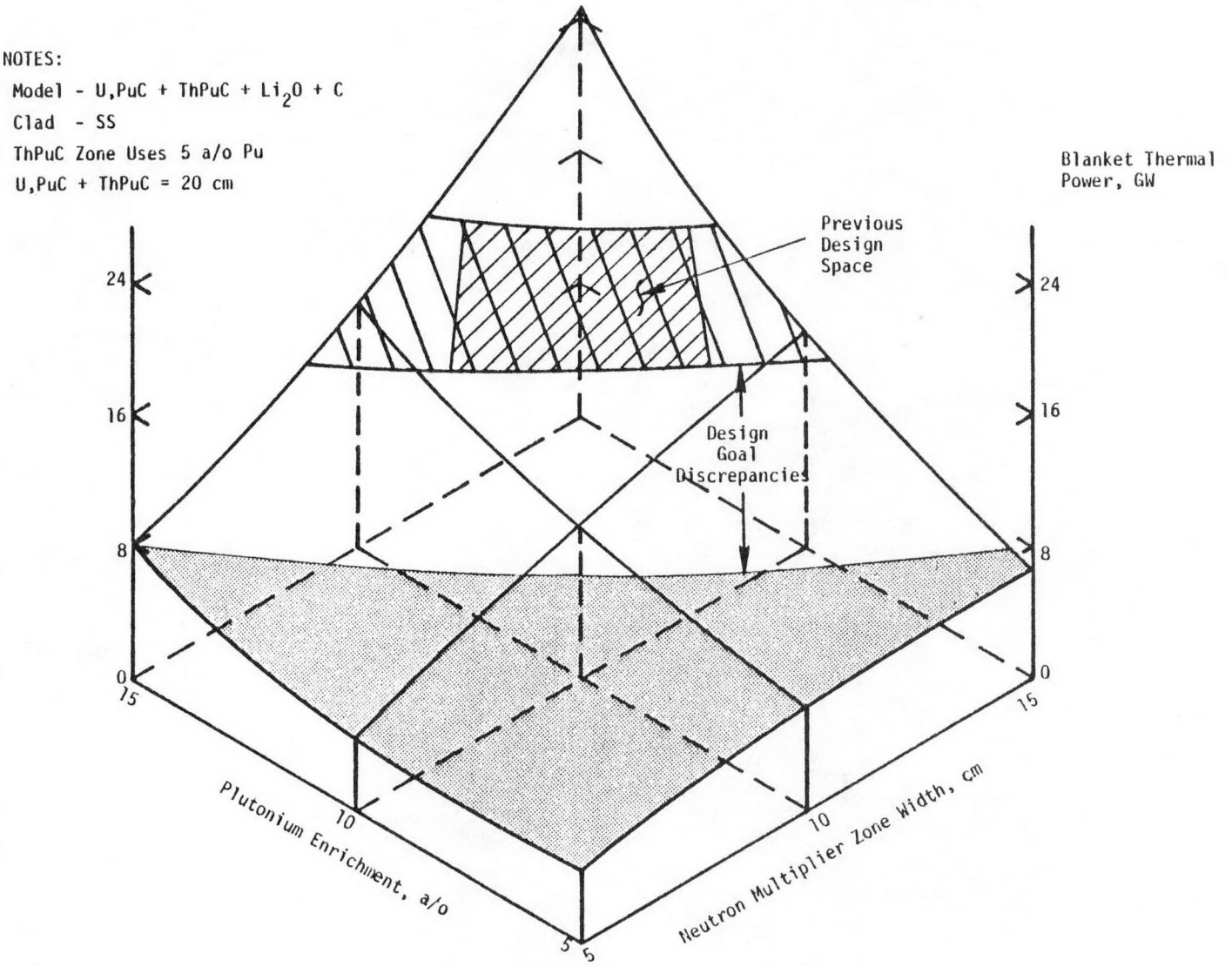

Figure 5-7. Blanket Thermal Power Versus Neutron Multiplier Width and Enrichment

Group C studies evaluated the general blanket performance for the condition where the tritium breeding zone was placed next to the plasma and the fissile breeding zone became the outboard area. The results are summarized in Table 5-6 and plotted surface responses are shown in Figure 5-8, 5-9, 5-10 and 5-11. As expected, the tritium breeding was consistently over 1.0 although the thickness (20 to 28 cm)* was not optimized with the 40.2% Li-6 enriched lithium material. Optimization of a practical design for this lithium zone appears feasible since the thinner cases (20 cm) showed slightly better T-breeding. The ^{233}U breeding was significantly reduced even with 15% Pu enrichment in the U, PuC neutron multiplier zone. It appears that a thicker multiplier zone or higher Pu enrichment would be necessary to improve ^{233}U breeding and thermal power. Evaluation of an Li_2O T-breeder zone next to the plasma with thicker fissile breeding zones may be worth exploring. Other changes such as using the less absorbant stainless steel clad instead of TZM may also be beneficial, as done in Group B.

Group D represents a study which might be labeled a "Pu Convertor" concept. This concept assumes that Pu is available from LWR discharge and can not be stored or recycled for LWR's, etc. Therefore, it must be burned up (fuel transmutation). Pu enrichment is permitted. The model retains the tritium breeding zone next to the plasma as in Group C except varies the Li-6 enrichment, eliminates U from the neutron multiplier zone and increases the enrichment of Pu to 30 to 40 a/o. The results are presented in Table 5-7 and are plotted in Figures 5-12 through 5-17. It can be seen that inventories of ~33 to 47 tonnes of Pu can be burned up at rates of 2.4 to 4.1 tonnes/yr while producing 3 to 5 tonnes/year of ^{233}U with thermal power outputs of 4 to 9 GW.** Tritium breeding self-sufficiency was achieved with 24 to 40% Li-6 enrichment. High fuel rod power densities were noted in some cases. Fuel rod power densities of 2400 W/cm^3 were assumed for EBR-II and ~2200 was used for FFTF. However, a specific coolant, fuel rod clad and fuel rod design would have to be analyzed to set this limit. While it is doubtful that applications involving such large Pu inventories would be of interest in the foreseeable future, the parametric trends shown do help to scope the upper limits of hybrid reactor performance capabilities. Case 13 depicts such a performance.

*Not all of the cases studied are shown in the Table.
**Data from Cases 4, 5, 7-9, and 15, which were the better all around performers.

TABLE 5-6

BLANKET PARAMETRIC CALCULATIONS - GROUP C

Case No. (f)	Blanket Zone Width, cm[a]			$\%^{235}U$ in U (c)	Pu Enrichment, a/o P_u(b)	Initial Inventory,[d] tonnes			Tritium Breeding Ratio	Fissile Production BOL-(tonnes/year)(e)		Blanket Thermal Power(e) (BOL) (GW)
	Tritium Breeder Li, 40% Li-6	Neutron Multiplier U, PuC	Fissile Breeder ThC			Pu	U	Th		^{233}U	^{239}Pu	
1	24	6	40	0.46	3.9	3.7	91	637	1.03	0.94	-0.30	1.05
3	20	10	40	0.25	5	7.9	149	637	1.02	0.97	-0.50	1.48
5	20	10	40	0.67	5	7.9	149	637	1.02	0.95	-0.50	1.53
6	24	6	40	0.20	10	9.5	85	637	1.04	0.97	-0.16	1.17
8	24	6	40	0.46	10	9.5	85	637	1.04	0.97	-0.16	1.18
9	19	10.9	40	0.46	10	17.2	154	637	1.06	1.09	-0.31	2.38
10	24	6	40	0.71	10	9.5	85	637	1.04	0.98	-0.16	1.19
12	20	10	40	0.25	15	23.7	134	637	1.10	1.20	-0.02	2.87
14	20	10	40	0.67	15	23.7	134	637	1.11	1.20	-0.02	2.93
15	24	6	40	0.46	16	15.3	79	637	1.07	1.05	-0.02	1.57

(a) Zones are NM-neutron multiplier; FB - Fissile Breeding; TB - Tritium Breeding. Order listed is closest to plasma first and then outward sequence. The fusion power source density is assumed to be 4 MW/m^2 at the first wall for all cases.

(b) Pu is assumed to be 69.6% fissile from LWR discharge. The Pu enrichment is in neutron multiplier zone.

(c) Natural U is ~0.7% ^{235}U; gaseous diffusion plant tailings are ~0.25% ^{235}U in U; other cases are mathematical selections.

(d) This group uses TZM clad.

(e) These values are at 100% plant capacity factor.

(f) All cases not shown had T-breeding zone of ~28 cm width, ~2 cm width neutron multiplier zone and only ~0.3 to 0.5 GW_t blanket power.

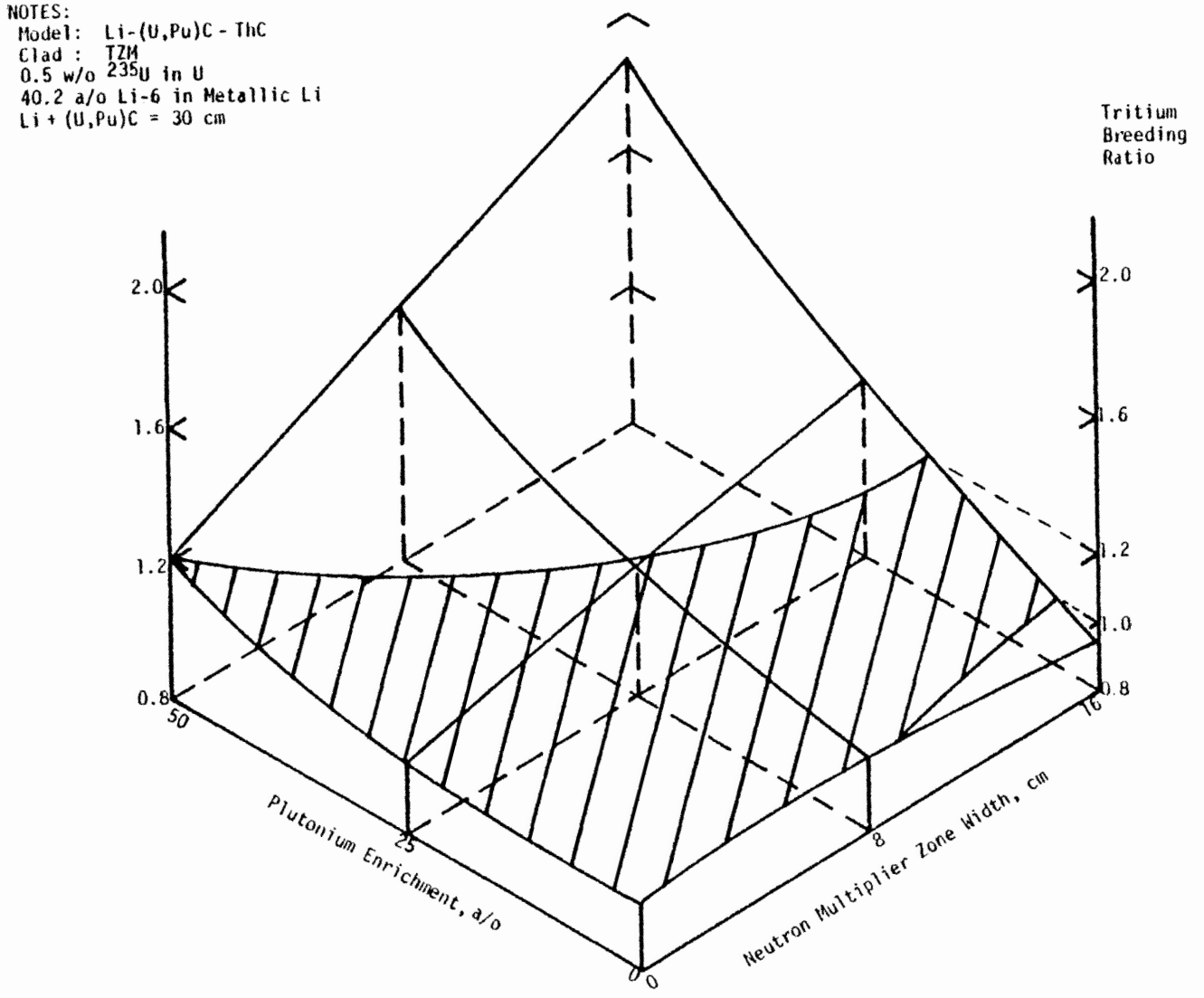

Figure 5-8. Tritium Breeding Ratio Versus Neutron Multiplier Width and Enrichment

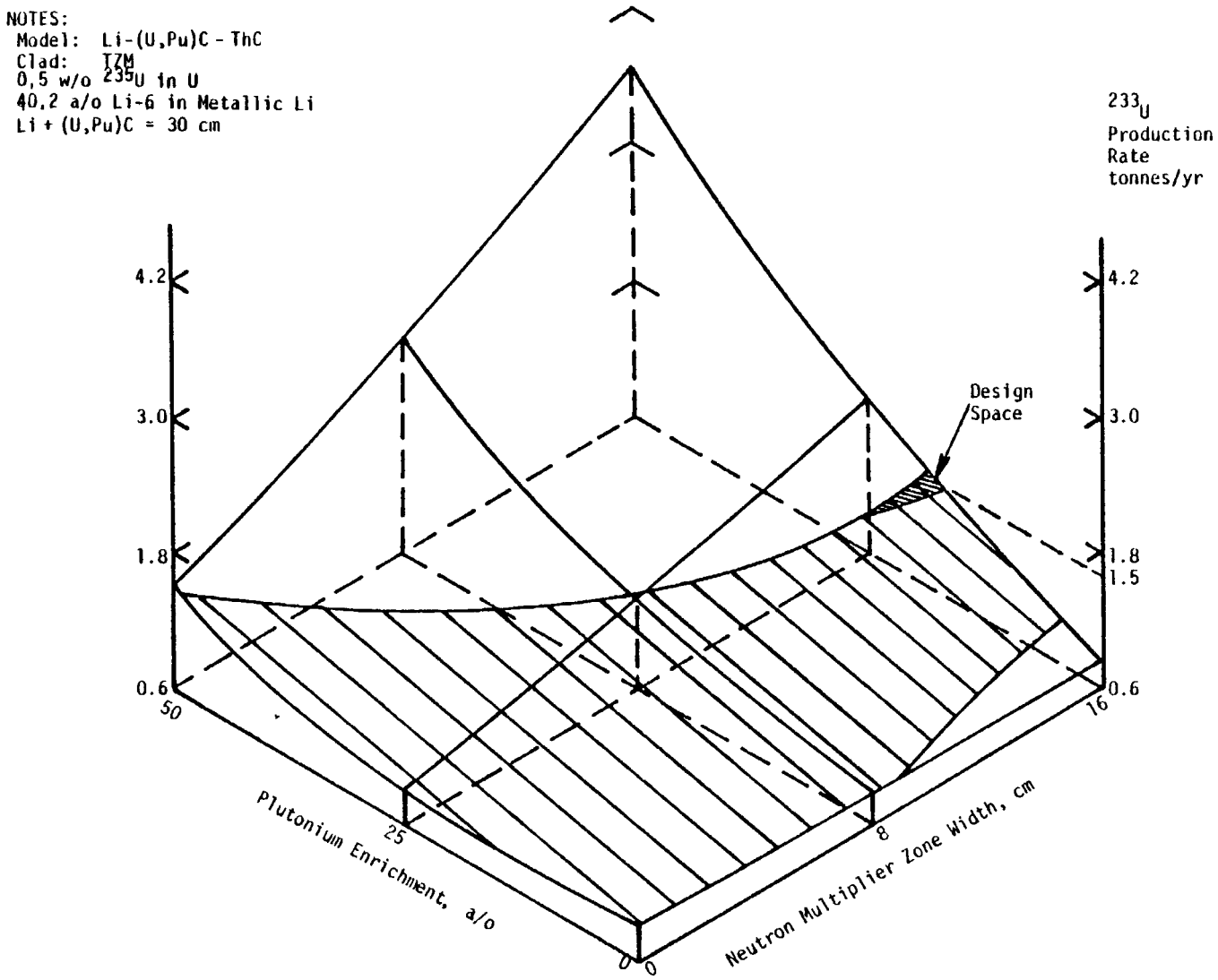

Figure 5-9. Uranium 233 Production Rate Versus Neutron Multiplier Width and Enrichment

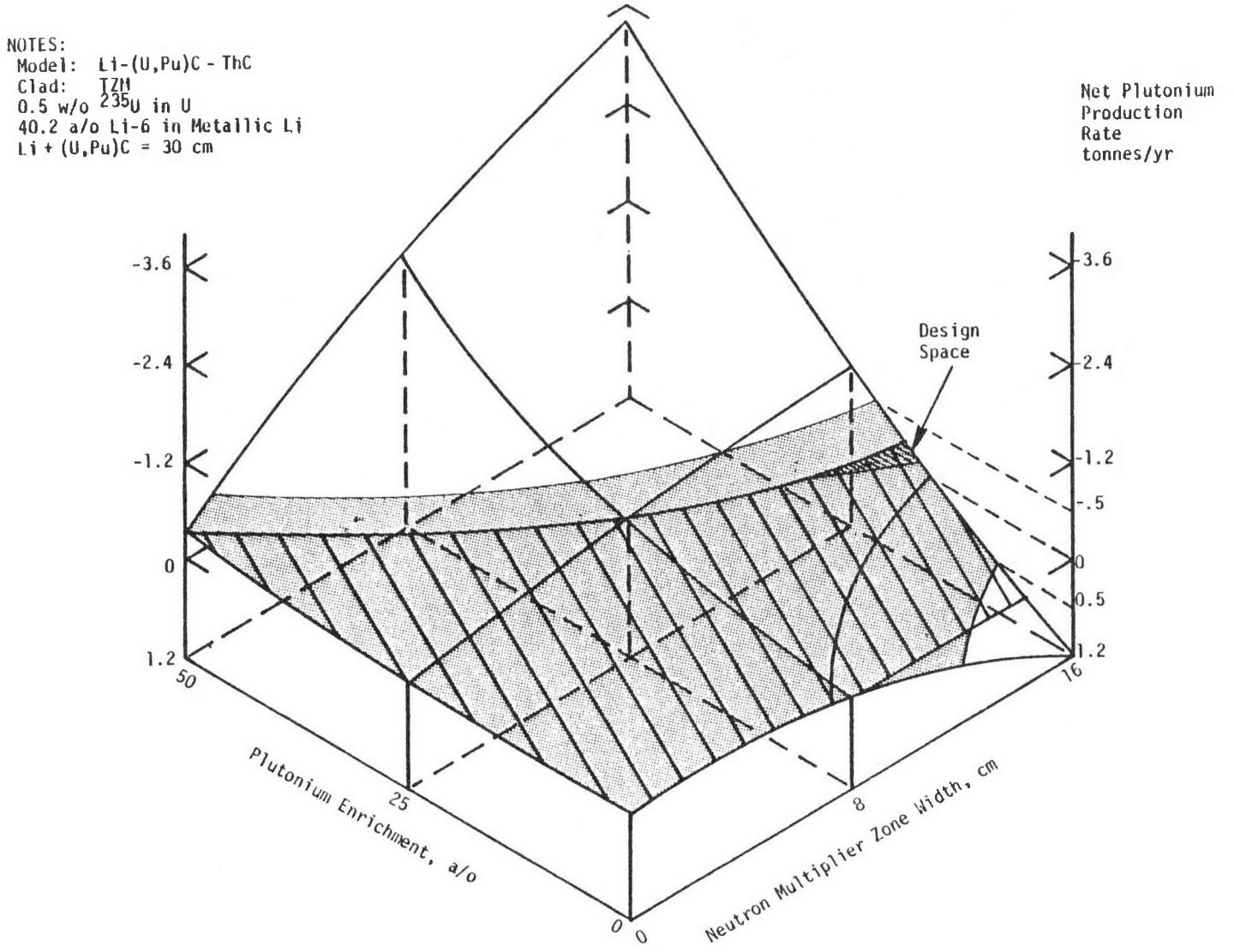

Figure 5-10. Plutonium Production Rate Versus Neutron Multiplier Zone Width and Enrichment

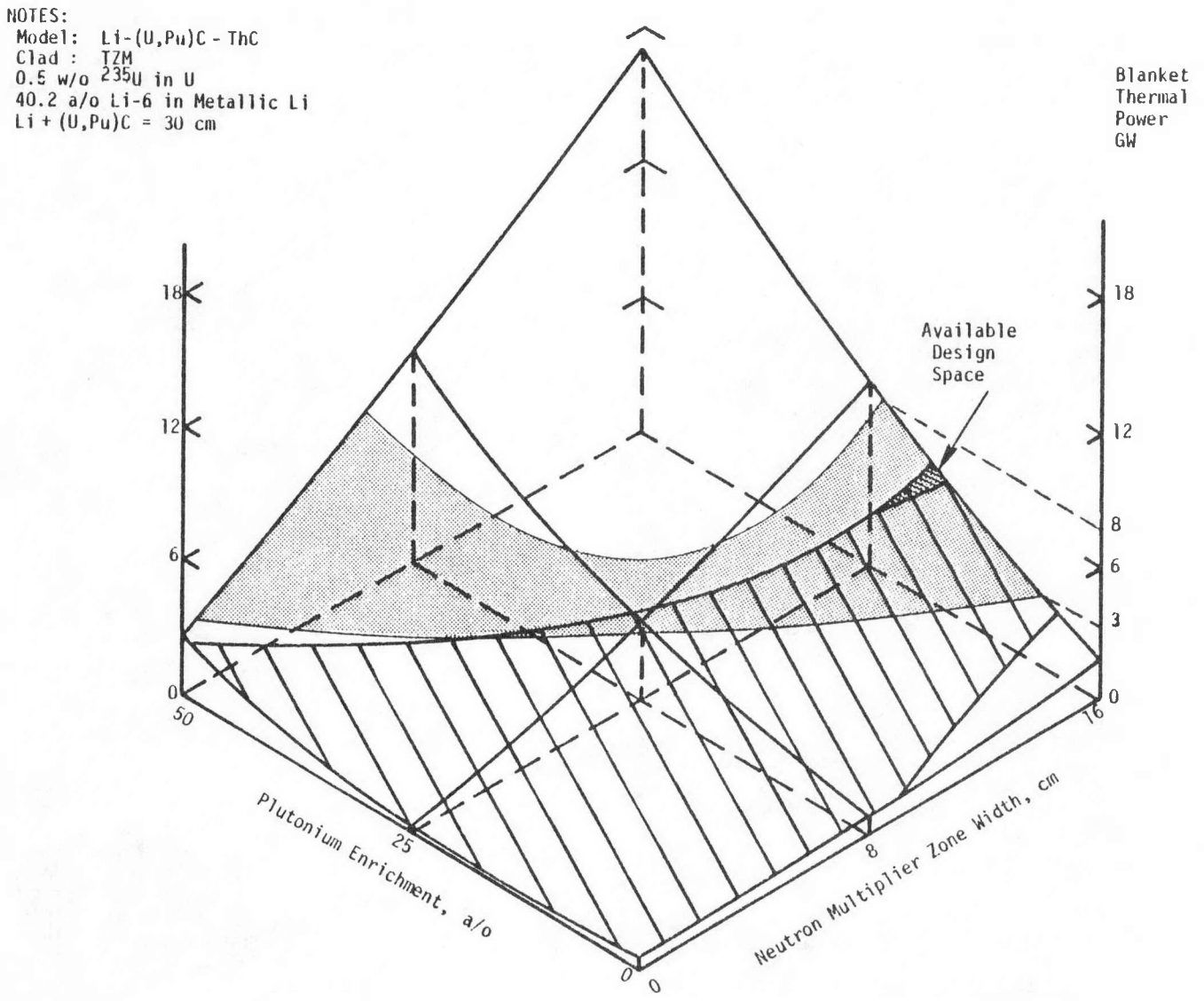

Figure 5-11. Blanket Thermal Power Versus Neutron Multiplier Zone Width and Enrichment

TABLE 5-7

PARAMETRIC CALCULATIONS - GROUP D

Case No.	Blanket Zone Width, cm[a]			% Li-6 in Li	Pu Enrichment, a/o P_u[b]	Initial Inventory,[d] tonnes			Tritium Breeding Ratio	Fissile Production BOL-(tonnes/year)[c]		Blanket Thermal Power[c] (BOL) (GW)	Max. Fuel Rod Power Density (W/cm^3)
	Tritium Breeder Li, Var Li-6	Neutron Multiplier Th, PuC	Fissile Breeder ThC/C			Pu	Th (NM zone)	Th (FB zone)		^{233}U	^{239}Pu		
1	14	6	30/20	23.9	28.9	27.0	64	572	1.00	3.2	-1.9	4.1	495
2	18	2	30/20	10.4	30	9.4	21	572	0.76	2.3	-0.9	1.6	472
3	18	2	30/20	37.3	30	9.4	21	572	0.93	2.0	-0.6	1.0	293
4	10	10	30/20	10.4	30	46.6	105	572	1.13	6.0	-3.9	17.0	1184
5	10	10	30/20	37.3	30	46.6	105	572	1.20	4.6	-2.8	9.1	667
6	18.9	1.1	30/20	23.9	35	6.2	11	572	0.89	2.0	-0.6	0.9	382
7	14	6	30/20	7.5	35	32.8	59	572	0.97	4.5	-3.5	8.4	1013
8	14	6	30/20	23.9	35	32.8	59	572	1.08	3.6	-2.8	5.5	648
9	14	6	30/20	40.2	35	32.8	59	572	1.11	3.3	-2.4	4.3	502
10	9.1	10.9	30/20	23.9	35	59.1	106	572	1.67	7.7	-5.0	22.6	1516
11	18	2	30/20	10.4	40	12.5	18	572	0.79	2.6	-1.7	2.1	652
12	18	2	30/20	37.3	40	12.5	18	572	0.95	2.1	-1.1	1.3	394
13	10	10	30/20	10.4	40	62.2	90	572	2.50	12.2	-7.5	55.6	4029
14	10	10	30/20	37.3	40	62.2	90	572	1.70	7.3	-5.6	19.3	1392
15	14	6	30/20	23.9	41	38.4	53	572	1.18	4.1	-4.1	7.2	840

(a) Zones are NM-neutron multiplier; FB - Fissile Breeding; TB - Tritium Breeding. Order listed is closest to plasma first and then outward sequence. The fusion power source density is assumed to be 4 MW/m^2 at the first wall for all cases.

(b) Pu is assumed to be 69.6% fissile from LWR discharge. The Pu enrichment is in neutron multiplier zone.

(c) These values are at 100% plant capacity factor.

(d) This group uses TZM clad.

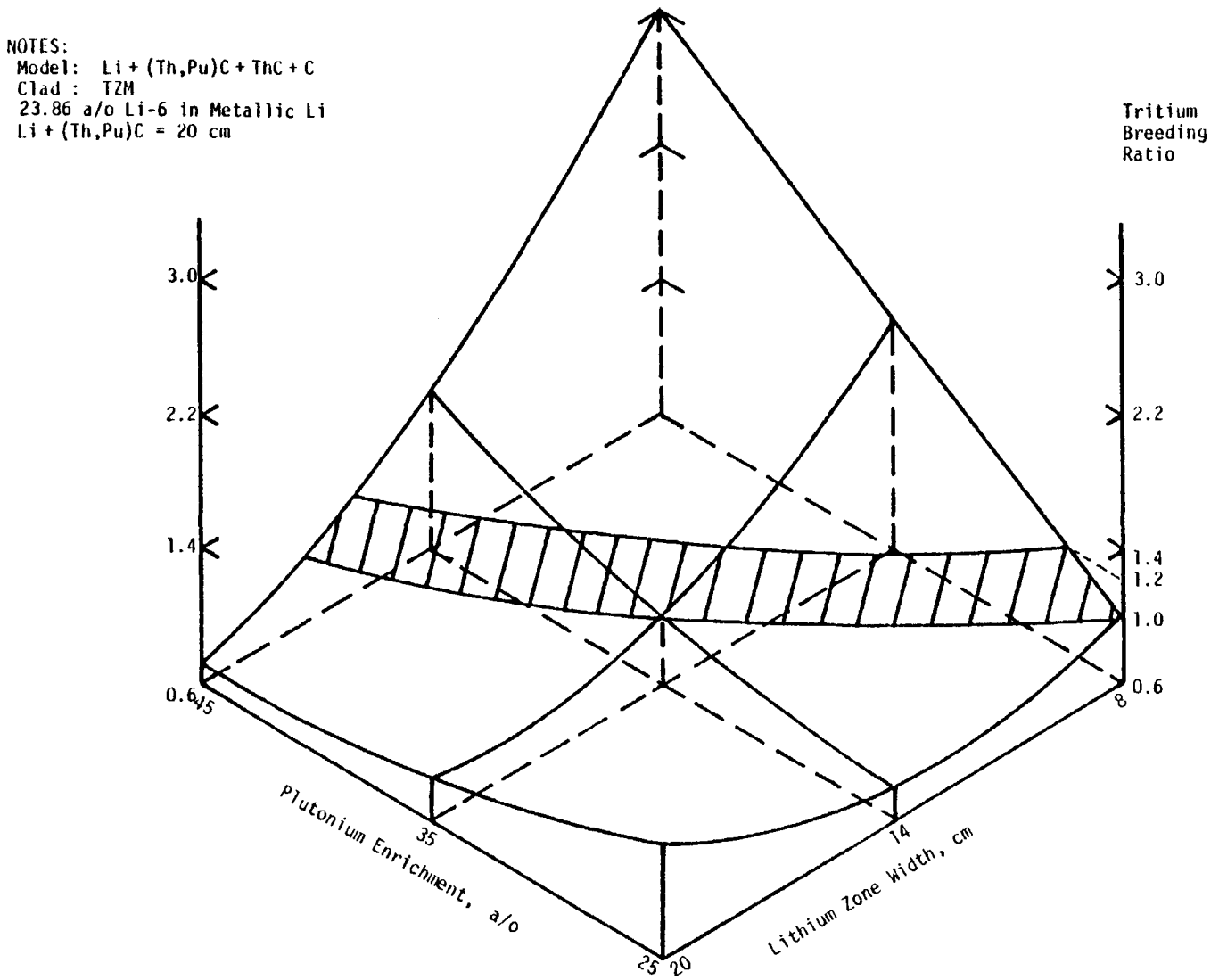

Figure 5-12. Tritium Breeding Ratio Versus Lithium Zone Width and Neutron Multiplier Enrichment

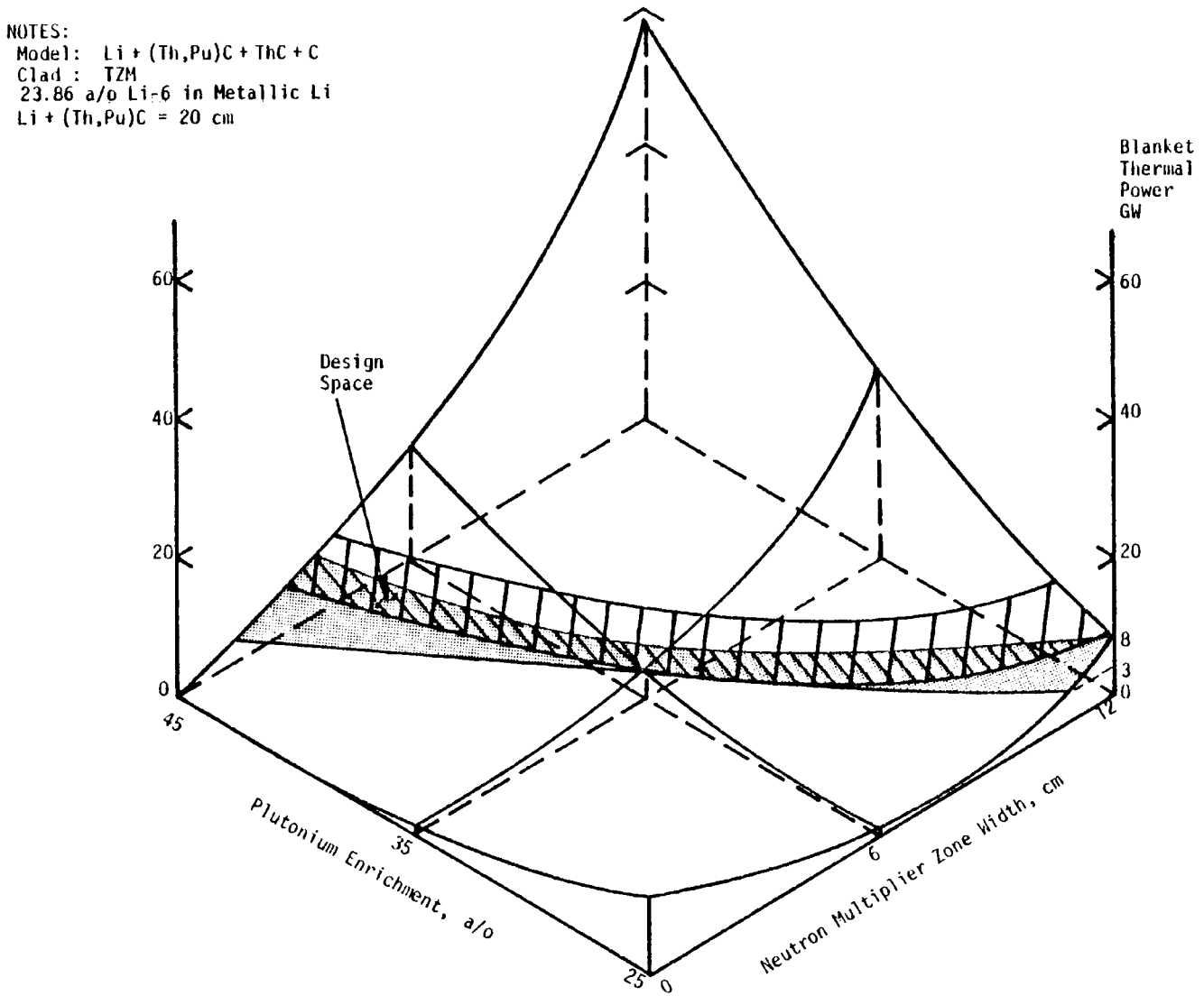

Figure 5-13. Blanket Thermal Power Versus Neutron Multiplier Width and Enrichment

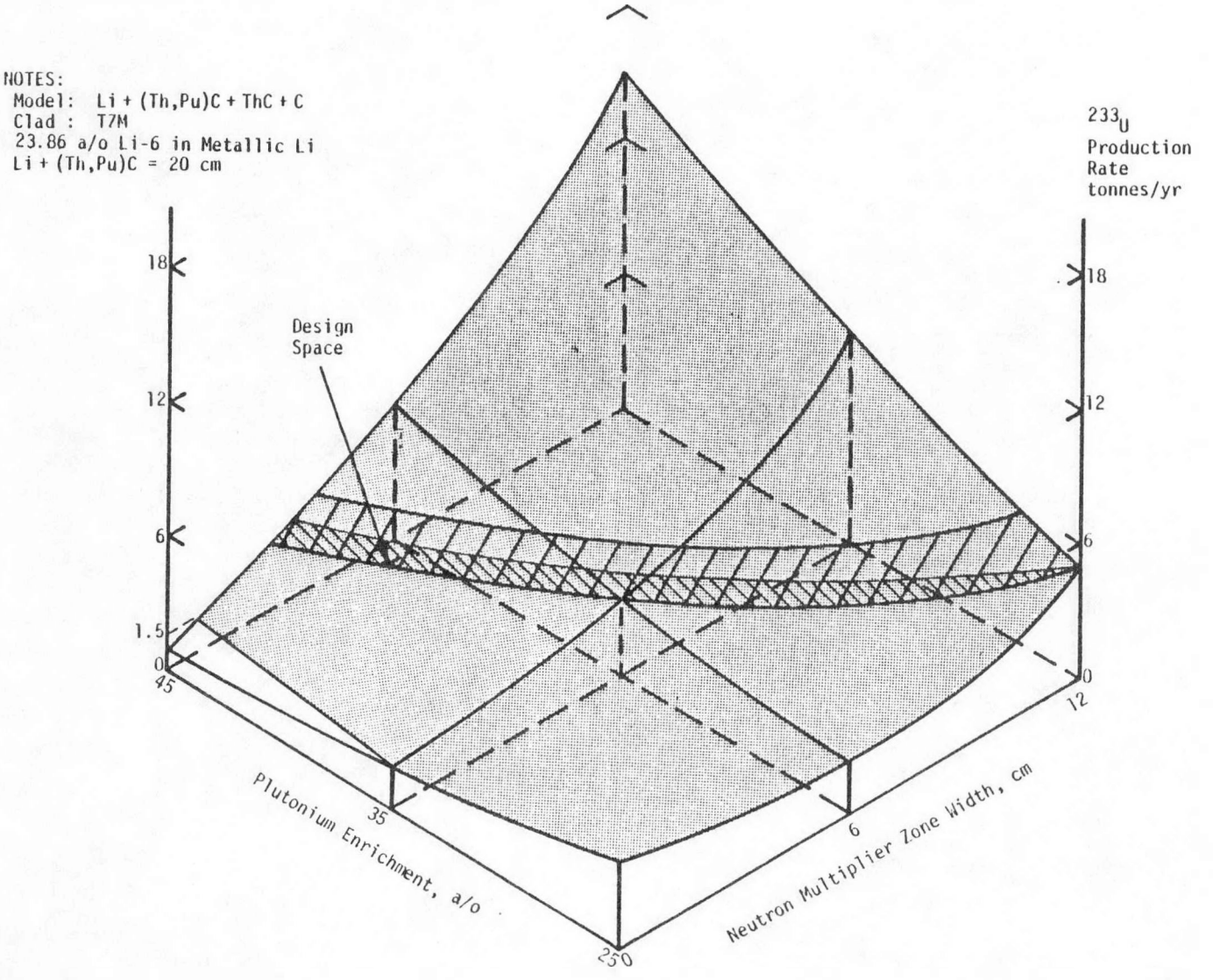

Figure 5-14. Uranium Production Rate Versus Neutron Multiplier Zone Width and Enrichment

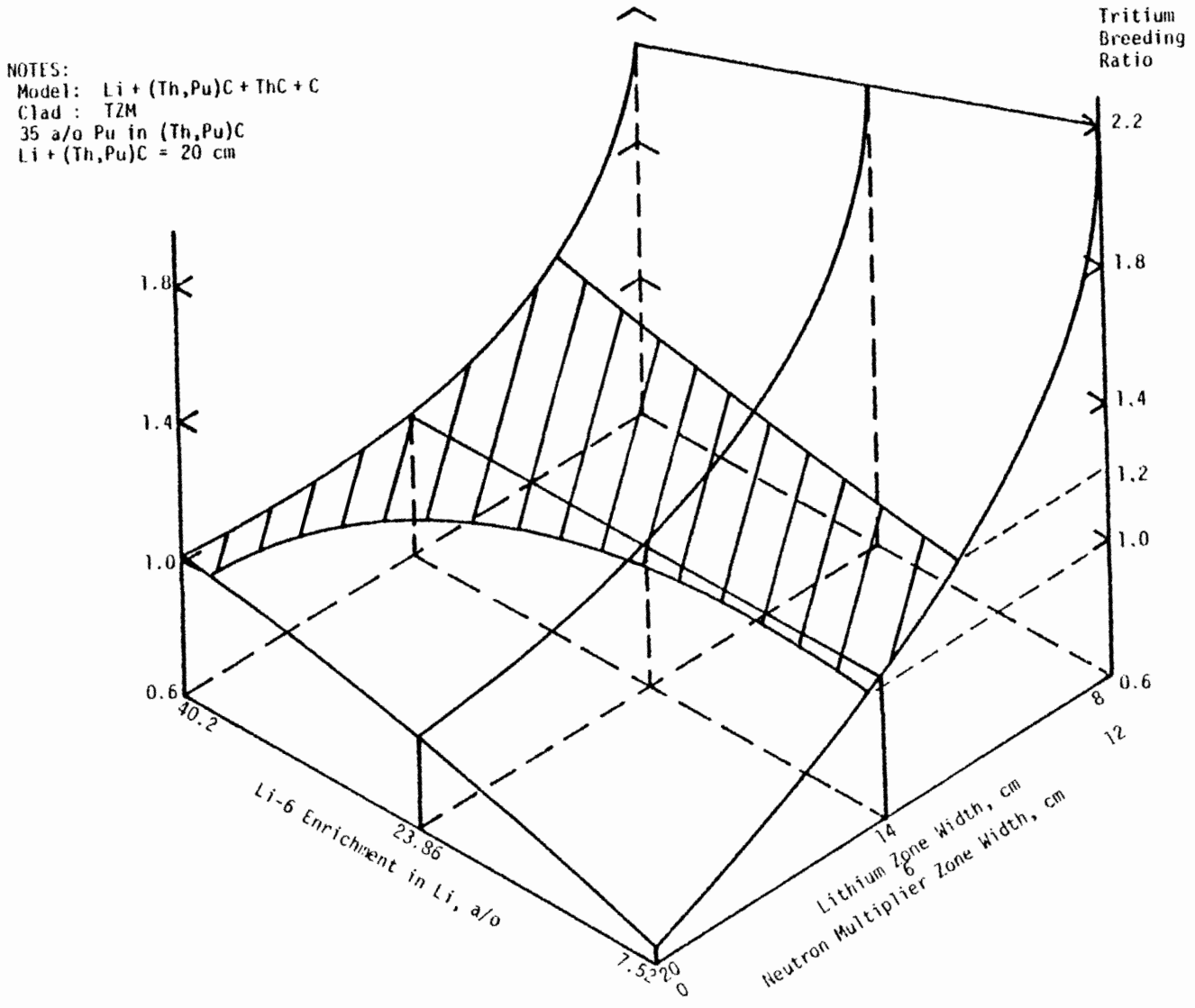

Figure 5-15. Tritium Breeding Ratio Versus Lithium Zone Width and Enrichment

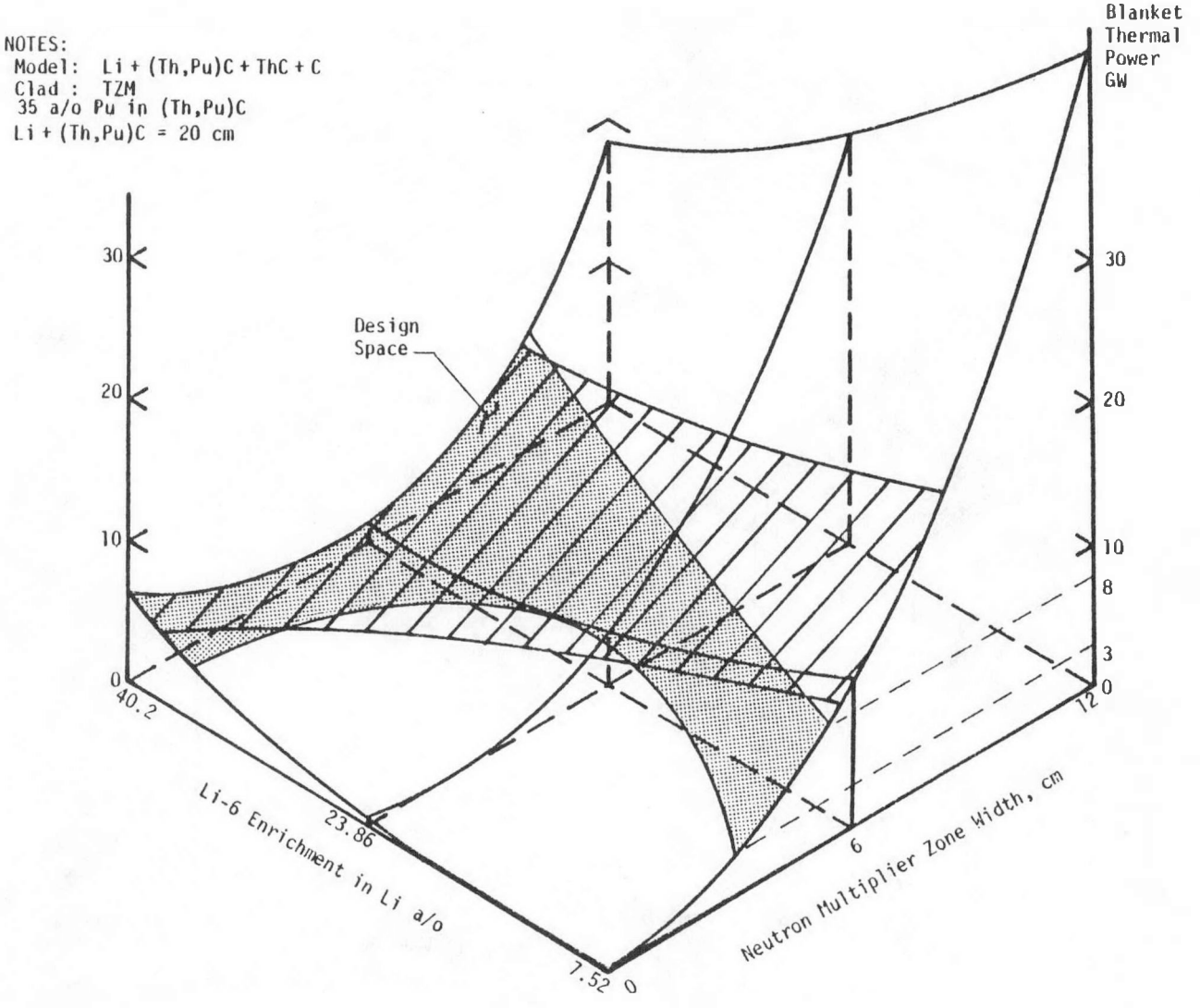

Figure 5-16. Blanket Thermal Power Versus Neutron Multiplier and Lithium Enrichment

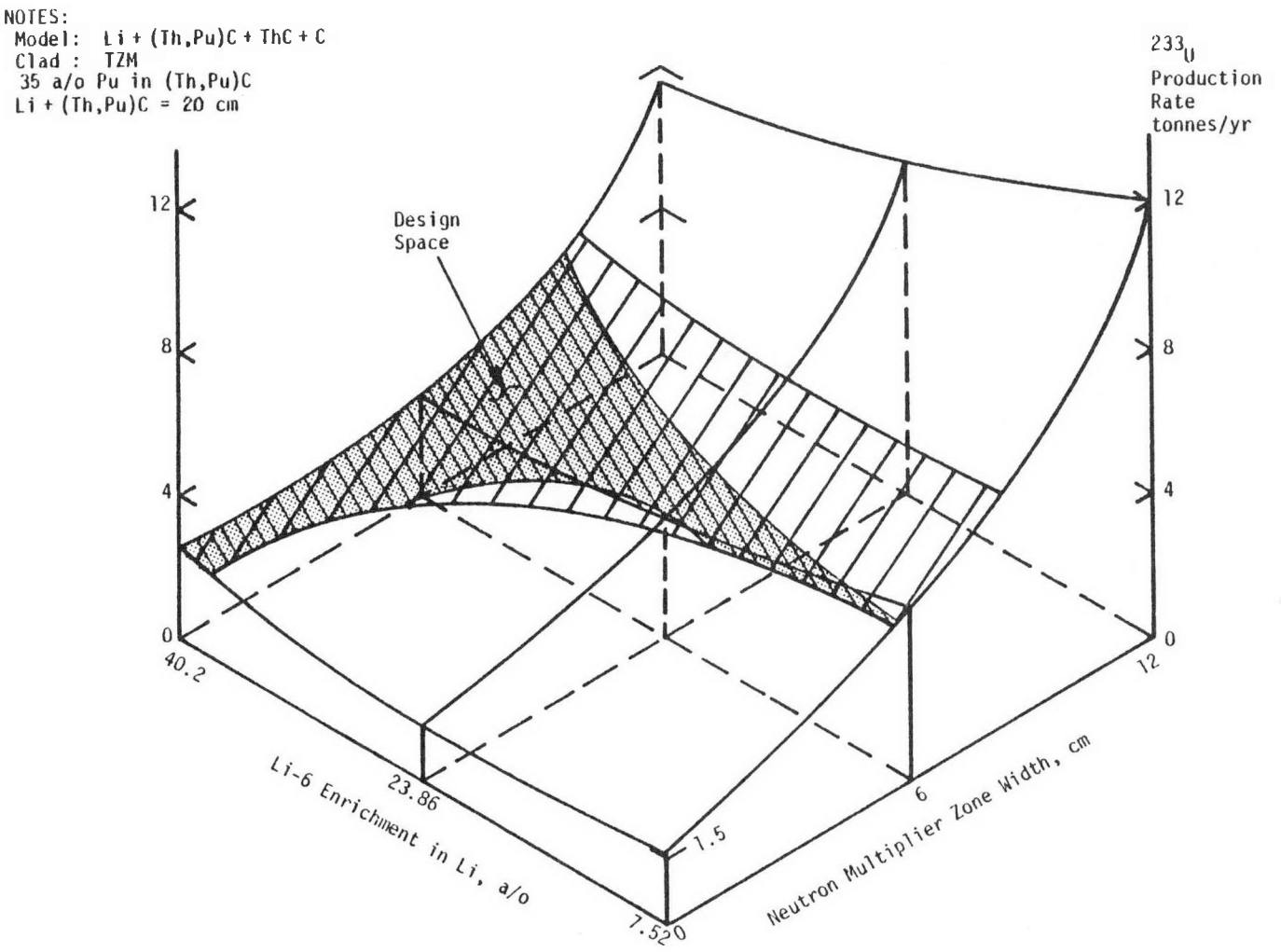

Figure 5-17. Uranium 233 Production Rate Versus Neutron Multiplier Width and Lithium Enrichment

5.3 NEUTRON WALL LOADING DISTRIBUTION

The variation of the fusion neutron wall loading about the torus of the tokamak hybrid reactor has been investigated in some detail. The results of the analysis are discussed in this subsection.

The poloidal variation of the wall loading is useful for several reasons. For example, it provides information on what fraction of the fusion neutron source passes through various sections of the first wall, such as the inner section where there may be no fissile blanket. It also provides information on the peaking of the wall loading at various positions on the wall. This is useful from a radiation damage standpoint as well as in indicating where more or less shielding may be necessary.

The basic tool used in the calculation was a computer code named WALLOAD, which allows a detailed three-dimensional calculation of the distribution of the angular and scalar neutron flux and current (wall load) around the wall of a tokamak fusion reactor. The effect of the toroidal geometry is implicitly included in the analysis by numerically solving the integral form of the neutron transport equation for streaming of neutrons from the plasma to the wall. The method uses a ray-tracing process which is essentially independent of the plasma source distribution and the shape of the first wall, so that it is applicable to nearly any tokamak reactor design. The code has been applied to several tokamak designs and is discussed further in Reference 14.

5.3.1 Application To The Hybrid Reactor

The WALLOAD code has been modified to facilitate analysis of various tokamak hybrid reactor designs. An elliptical shaped plasma and wall have been modeled for this first set of calculations, although this can be easily modified for future versions of the code once a "reference" design is selected.

The following parameters were used in the initial calculation to be consistent with the bundle divertor parameters in Section 4:

Major Radius, R_o	5.0 m
Plasma Half-Width, a_p	1.25 m

Wall Half-Width, a_w	1.40 m
Elongation Factor, K	1.6

All of the above parameters are input quantities to the code and hence, can easily be changed.

Three different elliptical plasma neutron source spatial distributions have been considered. The first is simply a uniform (constant) distribution throughout the plasma volume. The second source distribution is peaked at the plasma center and the volumetric source strength s (R, Z) is given by the equation

$$s\ (R, Z) = C \left(1 - \frac{\psi^2}{a_p^2}\right)^2 \tag{1}$$

where

$$\psi^2 = (R - R_o)^2 + \frac{Z^2}{K^2} \tag{2}$$

and C is a normalization constant. Here R and Z are the usual cylindrical coordinates. Note that this distribution has a maximum at the plasma center $(R_o, 0)$ and is zero at the plasma edge.

The third neutron source distribution used was both peaked and outwardly shifted to larger R values. This shifted source distribution is a fairly good representation of the outward shifting of the magnetic flux surfaces on which the plasma density and temperature, and therefore the neutron source, are nearly constant. Profiles of the shifted source strength are shown in Figure 5-18. The magnitude of the outward shift is given by the parameter ε, which can be approximated [15] by the expression

$$\varepsilon \simeq \frac{1 + 4\ \beta_p}{8A} \tag{3}$$

where β_p is the poloidal beta and A is the aspect ratio. For these calculations a value of $\varepsilon = 0.3$ was used; this value can be changed later when MHD equilibrium calculations are performed.

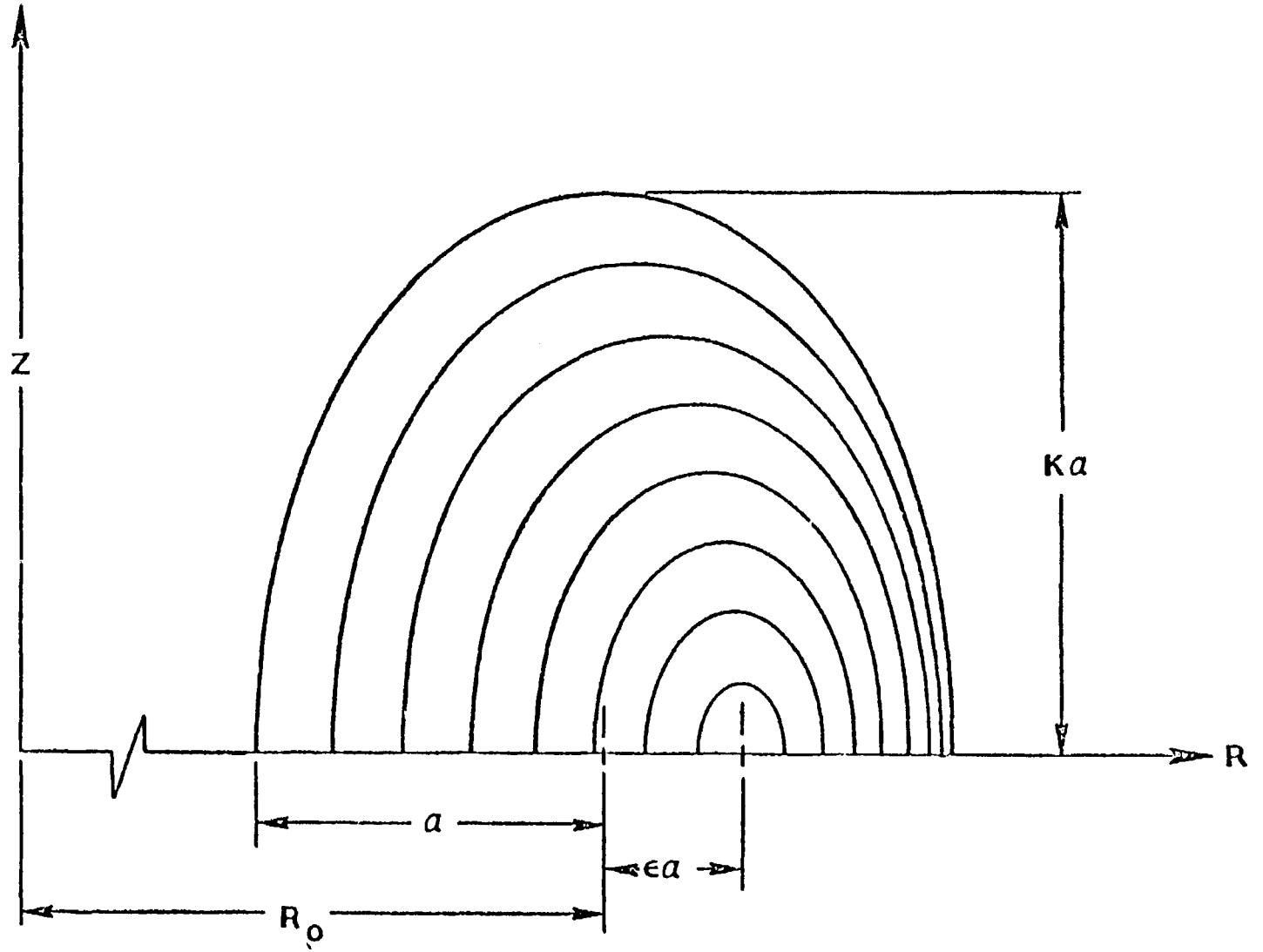

Figure 5-18. Profiles of the Shifted Neutron Source Strength

For all the calculations the three source distributions - uniform, peaked, and shifted - were normalized to the same total neutron source strength (plasma power).

5.3.2 Analysis Results

In Table 5-8 and Figure 5-19 the fraction of the source neutrons which strike different sections of the torus wall are given. For convenience the wall has been divided into 8 segments, denoted by letters A - H, with boundary heights in the Z direction of 0.5, 1.5, 2.0, and 2.24 m (top).

Table 5-8 shows that about 15.1% of the neutrons pass through wall section A for the shifted source, but it is only 12.7% for the uniform source and 13.7% for the peaked source. Similar differences are seen to occur at other wall sections. Note that all values in Table 5-8 apply to the wall section both above and below the midplane of the tokamak.

The fraction of neutrons which strike the inner blanket, divertor area and outer blanket for each of the sources can now be determined. Considering sections A-C as the outer blanket, D-E as the poloidal divertor area and F-H as the inner blanket, the totals become:

	Uniform Source	Peaked Source	Shifted Source
Outer Blanket (A-C)	51.6%	52.7%	55.7%
Divertor Area (D-E)	21.8%	20.0%	19.5%
Inner Blanket (F-H)	26.6%	27.3%	24.8%

The shifted plasma source model is probably the most realistic and hence, the results indicate that about 20% of the fusion neutrons will be lost in the divertor region (if a poloidal divertor is used) and only about 25% will strike the inner blanket.

The fact that only 25% of the fusion neutrons strike the inner blanket is the reason for the difficulty that has been encountered in breeding sufficient tritium from this area alone. Some Li bearing zones must also be put on the outer and top areas of the blanket in order to breed enough tritium.

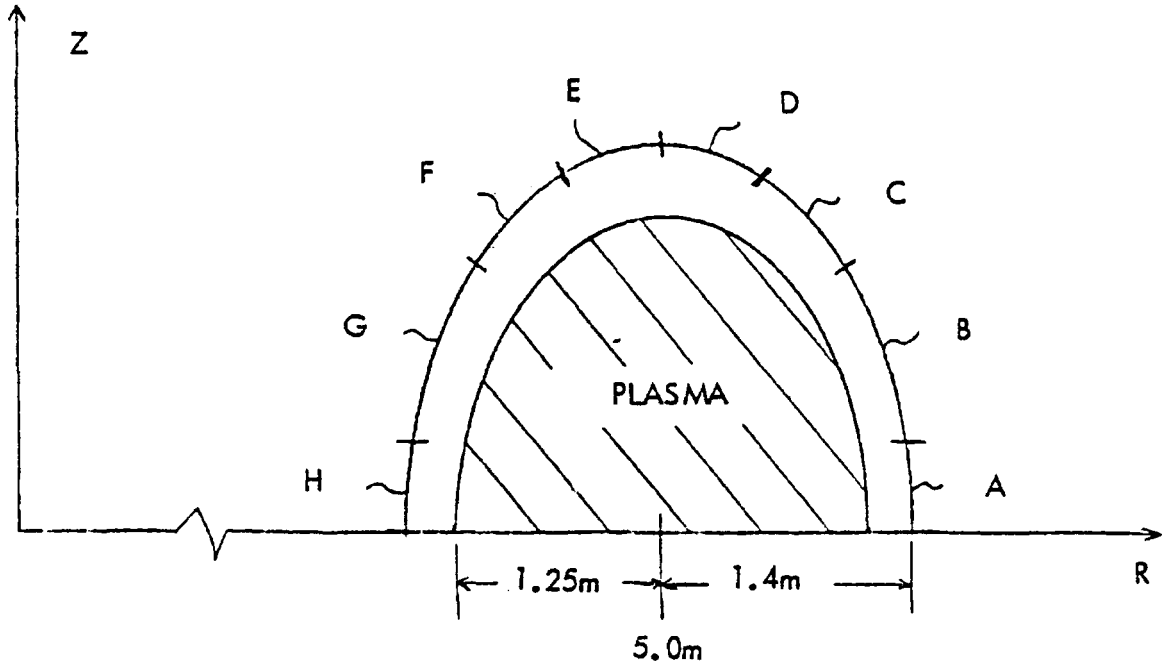

Figure 5-19. Cross Section of Elliptical First Wall and Definition of Wall Segments

Table 5-8. Fraction of Fusion Neutrons Striking Various Wall Segments

Wall Section	Upper Height Z (m)	Percent of the Fusion Neutron Source Passing through the Wall Section		
		Uniform Source	Peaked Source	Shifted Source
A	0.5	12.7%	13.7%	15.1%
B	1.5	25.3%	26.0%	27.6%
C	2.0	13.6%	13.0%	13.0%
D	2.24	12.2%	11.3%	11.0%
E	2.24	9.6%	8.7%	8.5%
F	2.0	8.1%	7.6%	7.2%
G	1.5	12.6%	13.1%	11.8%
H	0.5	5.9%	6.6%	5.8%
	TOTAL:	100.0%	100.0%	100.0%

It should be noted that these calculations are only of the uncollided, virgin 14 MeV fusion neutron wall distribution. There will, of course, be some neutron production in the outer (fission) blanket which will result in more neutrons striking the inner wall. However, these would be lower energy neutrons with higher probability of reflection from the inner wall. This situation can only be analyzed with a two-dimensional transport calculation such as with DOT. Nonetheless, these wall load calculations are of interest in understanding how the fusion neutrons are distributed about the first wall.

From Table 5-8 we can also make an estimate of the fraction of the neutrons lost due to holes in the first wall for neutral beam injectors or a bundle divertor. Considering wall section A on the first wall, the total wall area covered by this strip 1.0 m wide (0.5 m above and below the midplane) is $2\pi \times 6.4 \times 1 = 40.2\ m^2$. For the shifted source, 15.1% of the neutrons strike this area; and thus for an area of 1 m^2 the fraction of source neutrons lost is

$$\frac{0.151}{40.2} \times 1.0 \simeq 0.004$$

Thus, for each hole of area 1 m^2 on the outer wall there is a loss of about 0.4% of the fusion neutrons.

A second quantity of interest is the actual magnitude of the neutron wall loading, J about the wall, especially to determine where the peaking is most severe. The wall load peaking factor is plotted versus wall position (as determined by the R coordinate) in Figure 5-20 Here the wall load peaking factor is defined as the ratio of the wall loading at a certain point to the nominal wall loading J_{nom}, where J_{nom} is the total plasma fusion neutron power divided by the wall area.

Figure 5-20 shows a strong dependence of the peaking factor on the plasma spatial distribution. The peaking can be as high as 40% for the shifted source on the outer wall to as low as about 0.76 times nominal part way up the inner wall. The overall peaking is less severe for the uniform source than for the peaked and shifted sources.

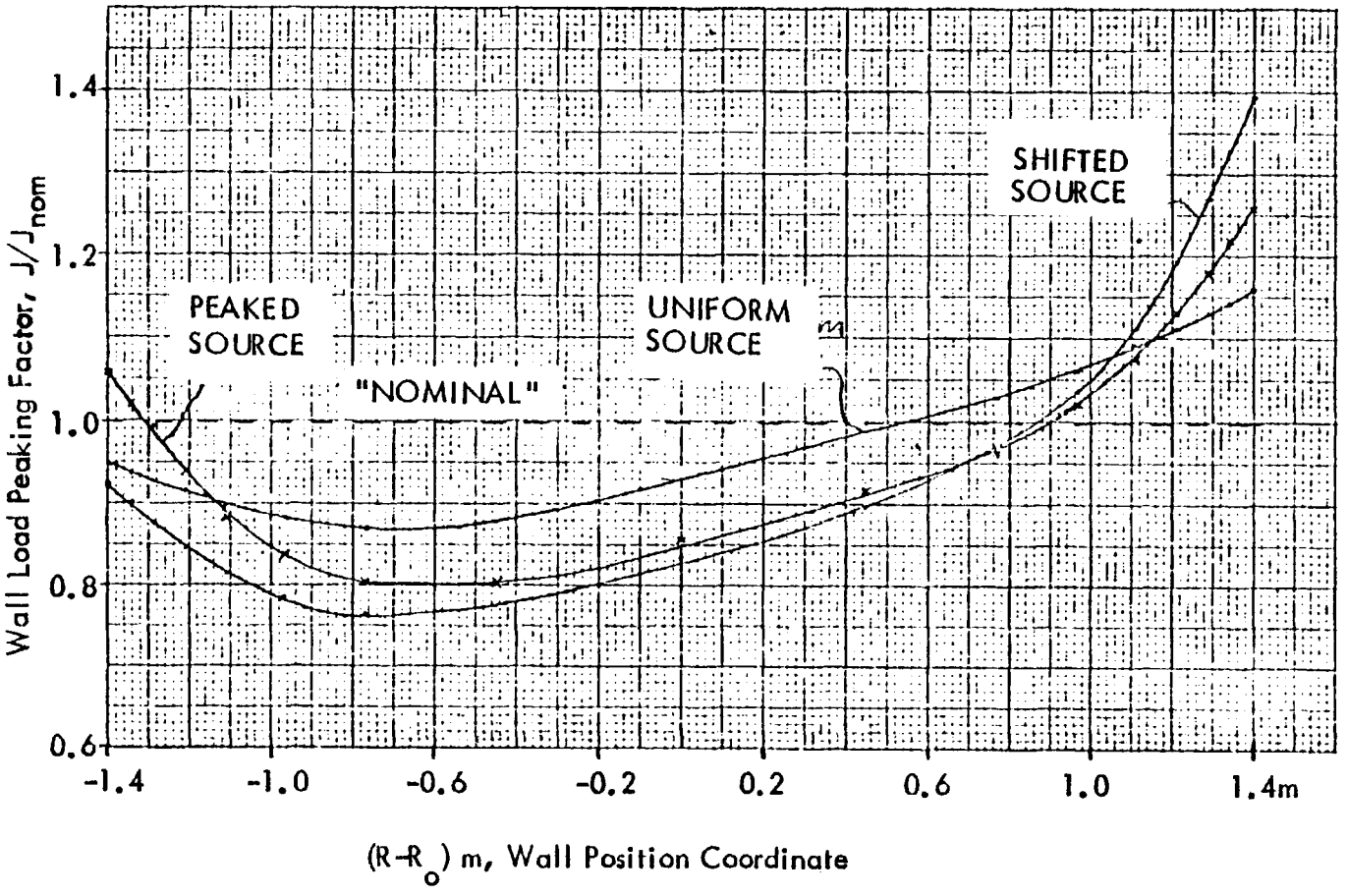

Figure 5-20. Variation of the Neutron Wall Loading about the First Wall for Three Plasma Source Distributions

If the hybrid breeder is designed with a nominal wall loading of 3.0 MW/m^2, then for the shifted source (which is most realistic) the wall load at the outermost point will be about 1.4 x 3.0 = 4.2 MW/m^2. This high a value could have a considerable effect on the cooling requirements and structural integrity of the wall at this point due to excessive heat generation and radiation damage.

At the innermost wall point, the wall load is about 93% of nominal indicating a possible reduction in the inner side shield thickness requirement. This may not seem like a great amount, but the peaking is even lower at other points on the inner wall indicating further potential for reductions in the amount of shielding. As is well known, any space on the inner side of the torus is very valuable and a thinner shield could result in a significant cost reduction.

5.3.3 Summary

The fusion neutron wall load distribution for a tokamak hybrid reactor design has been evaluated. Estimates of the source fraction striking various wall segments have been made as well as of the peaking factor about the wall. Now that the WALLOAD code is operational, similar calculations can be performed in more detail in the future for various reference design configurations. Future analyses could also include the angular variation of the neutron flux at various wall points.

6.0 REFERENCES

1. "Preliminary Assessment of Nuclear Proliferation as it Pertains to Fusion Power," WFPS-TME-046, October 1977, Westinghouse Fusion Power Systems Department, Pittsburgh, PA (to be issued).

2. "Engineering Parameters for Four Ignition TNS Tokamak Reactor Systems," WFPS-TME-058, September 30, 1977, Westinghouse FPSD, Pittsburgh, PA.

3. Rose, R. P. et al., "Fusion Driven Actinide Burner Design Study," EPRI Report No. ER-451 (Vol. I and II) May 1977 (Westinghouse Fusion Power Systems Department, Pittsburgh, PA).

4. Rose, R. P. et al., "Fusion-Driven Breeder Design Study," Final Report, WFPS-TME-043, May 1977, Westinghouse Fusion Power Systems Department, Pittsburgh, PA (to be issued).

5. Yang, T. F., "A Consideration of a Bundle Divertor Design for TNS," WFPS-TN-076, (June, 1977) Westinghouse Fusion Power Systems Department, Pittsburgh, PA.

6. Paul, J. W. M., et al., IAEA 6th Conf. on Plas. and Control Nucl. Fus. Research, IAES-CN-35/A17, Berchtesgaden, FRG (October, 1976).

7. TNS Engineering Quarterly Progress Report, WFPS-TN-061 (January-February-March, 1977), Westinghouse Fusion Power Systems Department, Pittsburgh, PA.

8. Yang, T. F. and G. A. Emmert, Proc. of 1st Topical Meeting on Tech. of Control Nucl. Fusion, Vol. 2, San Diego, CA (1974) 400.

9. Kirst, D. W., UWPLP-613 (1975) "Electric Field Effects in Our Octupoles and Application to Divertors and Limiters," University of Wisconsin Internal Report.

10. Schmidt, George, Physics of High Temperature Plasmas, Academic Press, N.Y. (1960), p. 160.

11. Moir, R. W. and W. L. Barr, "Venetian-Blind Direct Energy Convertor For Fusion Reactors," Nuclear Fusion Vol. 13, p. 35 (1973).

12. Fortescue, P., "Comparative Breeding Characteristics of Fusion and Fast Reactors," Science 196, 1326 - 29, June 17, 1977.

13. Krase, J. W. and C. Cyl-Champlin, "Synthetic Experiment Design Techniques in Reactor Analysis," APEX-303, May 1957.

14. Chapin, D. L. and W. G. Price, Jr., Nucl. Tech. 31, 32 (1976).

15. Greene, J. M., J. L. Johnson and K. E. Weimer, Phys. Fluids 14, 671 (1971).